ESA Climate Change Initiative (CCI)

Sea Level Budget Closure (SLBC_cci)

Sea Level Budget Closure Assessment Report
ESA_SLBC_cci_D3.1
Version 1.1, issued May 07, 2018

SLBC Assessment Report 1 based on version 0 data

Prime & Science Lead:	Martin Horwath
	Technische Universität Dresden (TUDr)
	Martin.Horwath@tu-dresden.de
Technical Officer:	Jérôme Benveniste
	ESA ESRIN, Frascati, Italy
	Jerome.Benveniste@esa.int
Consortium:	Laboratoire d'Etudes en Géophysique et Océanographie Spatiales (LEGOS)
	Universität Bremen (UB)
	Universität Zürich (UZH)
	University of Leeds (UoL)
	Goethe-Universität Frankfurt (GUF)
	Danmarks Tekniske Universitet, DTU Space, Geodynamics (DTU-GDK)
	Danmarks Tekniske Universitet, DTU Space, Geodesy (DTU-GEK)
	Nansen Environmental and Remote Sensing Center (NERSC)
	University of Reading (UoR)
	Mercator Ocean, Toulouse (MerO)

To be cited as:
Novotny, K.; Horwath, M.; Cazenave, A.; Palanisamy, H.; Marzeion, B.; Paul, F.; Döll, P.; Cáceres, D.; Hogg, A.; Shepherd, A.; Forsberg, R.; Sørensen, L.; Barletta, V.R.; Andersen, O.B.; Ranndal, H.; Johannessen, J.; Nilsen, J.E.; Gutknecht, B.D.; Merchant, Ch.J.; MacIntosh, C.R., von Schuckmann, K.: *ESA Climate Change Initiative (CCI) Sea Level Budget Closure (SLBC_cci) Sea Level Budget Closure Assessment Report D3.1. Version 1.1, 07.05.2018.*

Signatures page

Prepared by	Kristin Novotny Project Manager, TUDr Martin Horwath Science Leader, TUDr Anny Cazenave, Hindumathi Palanisamy, LEGOS; Ben Marzeion, UB; Frank Paul, Raymond Le Bris, UZH; Petra Döll, Denise Cáceres, GUF; Anna Hogg, Andrew Shepherd, UOL; Rene Forsberg, Louise Sandberg Sørensen, DTU-GDK; Ole B. Andersen, Heidi Ranndal, DTU-GEK; Johnny Johannessen, Jan Even O. Nilsen, NERSC; Benjamin D. Gutknecht, TUDr; Christopher John Merchant, Claire Rachel MacIntosh, UoR; Karina von Schuckmann, MerO	Date: 2018-05-07
Checked by	Martin Horwath Science Leader, TUDr	Date: 2018-05-08 Martin Horwath
Approved by	Jérôme Benveniste Technical Officer, ESA	Date:

Change Log

Issue	Author, Org.	Affected Section	Reason/Description	Status
1.0	M. Horwath / TUDr …	All	Document Creation	Released to ESA 2018-02-05
1.1	M. Horwath / TUDr …	All	Document Revision after review by ESA	Released to ESA 2018-05-08

Distribution List

Organization	Consortium Member
TUDr	Martin Horwath
LEGOS	Anny Cazenave
UB	Ben Marzeion
UZH	Frank Paul
UoL	Andrew Shepherd, Anna Hogg
DTU- GDK	Rene Forsberg
GUF	Petra Döll
NERSC	Johnny Johannessen
DTU-GEK	Ole B. Andersen
UoR	Christopher Merchant
MerO	Karina von Schuckmann
ESA	Jérôme Benveniste Marco Restano Américo Ambrózio

Table of Contents

Acronyms and Abbreviations

Acronym	Explanation
AIS	Antarctic Ice Sheet
AVISO	Validation and Interpretation of Satellite Oceanographic data
CCI	Climate Change Initiative (initiated by ESA)
CRU	Climatic Research Unit (University of East Anglia, Norwich, UK)
CRUGPCC	combined climatology data from CRU (temperature, cloudiness, number of days with rain) and GPCC (precipitation)
CSIRO	Commonwealth Scientific and Industrial Research Organization
CSR	Center for Space Research (University of Texas at Austin)
DTU	Danmarks Tekniske Universitet
ECMWF	European Centre for Medium-Range Weather Forecasts
EN4	version 4 of the Met Office Hadley Centre ''EN'' series of data sets of global quality controlled ocean temperature and salinity profiles
ERA	Earth system ReAnalysis
ESA	European Space Agency
e.s.l.	equivalent sea level
EWH	equivalent water height
GFZ	GeoForschungsZentrum Potsdam
GIA	Glacial Isostatic Adjustment
GIS	Greenland Ice Sheet
GMB	Gravimetric Mass Balance / GRACE Mass Balance
GMBAL	Global Glaciology: Mass Balance of Small Glaciers (dataset containing all available time series of annual and multi-annual mass balance measurements for the small glaciers of the world)
GMSL	Global Mean Sea Level
GPCC	Global Precipitation Climatology Centre
GRACE	Gravity Recovery and Climate Experiment
GrIS	Greenland Ice Sheet
GRS-80	Geodetic Reference System 1980,
GSFC	Goddard Space Flight Center
GSSL	Global mean Steric Sea Level
IB	Inverse Barometer
ICE-4, ICE-5G, ICE-6G_C	models of postglacial relative sea-level history
IK	steric sea level data set by Ishii and Kimoto (2009)
IMBIE	Ice Sheet Mass Balance Inter-comparison Exercise
IPRC	International Pacific Research Center
ISBA	Interaction Soil Biosphere Atmosphere
ITSG	Institute of Geodesy, Theoretical Geodesy and Satellite Geodesy (TU Graz)
JAMSTEC	Japan Agency for Marine-Earth Science and Technology
JPL	Jet Propulsion Laboratory

KVS	Updated version of the global mean steric time series computed by von Schuckmann and Le Traon (2011)
LEGOS	Laboratoire d'Etudes en Géophysique et Océanographie Spatiales
LWS	Land Water Storage
NOAA	National Oceanographic and Atmospheric Administration
OBP	Ocean Bottom Pressure
OMC	Ocean Mass Change
R1501	GMBAL Release 1501
SCRIPPS	Scripps Institution of Oceanography (University of California)
SLA	sea level anomaly
SLE	Sea Level Equivalent
SL_cci	ESA CCI_Sea Level Project
SLB	Sea Level Budget
SLBC	Sea Level Budget Closure
SLR	Satellite Laser Ranging
SSH	Sea Surface Height
STD	Standard Deviation
TBE	To Be Established
TOPAZ	(Towards) an Operational Prediction system for the North Atlantic European coastal Zones
TRIP	Total Runoff Integrating Pathways
TUDr	TU Dresden
TWS	Total Water Storage
TWV	Atmospheric Water Vapor
v0	SLBC_cci version 0 data of individual components as described in the SLBC_cci Product Description Document D2.1.2
VM	model of the radial viscoelastic structure of the Earth (used fo ICE-models)
w.e.	water equivalent
WFDEI	Watch Forcing Data based on ERA-Interim reanalysis
WGHM	WaterGAP Global Hydrology Model
WP	Work Package
XBT	Expendable Bathythermograph

1 Introduction

1.1 Purpose and Scope

This document discusses the results of the sea level budget closure assessment at the beginning stage of the project. The comparisons and results are based on the version 0 (v0) data as they are described in detail in the SLBC_cci Product Description Document D2.1.2 (see below). Some improvements made since the v0 data delivery in June 2017 were included into this report (Section 2). In addition, some more external data were used for comparison and quality control to the v0 data.

V0 data and products have been gathered in the initial phase of the SLBC_cci project to reflect the situation at the beginning of the project, prior to any improvement and further adaptation. Therefore, the budget closure assessment discussed here also shows the situation at the project's starting point and already gives some implications for further improvements and scientific questions within the SLBC_cci project. The results were discussed within the entire consortium during the project meeting in October 2017, at the monthly telecons and in numerous bilateral discussions.

Due to the different progress in the different WPs, owing to differences in the data situation, some differences in length and detail between the chapters exist. Some repetitions of ocean mass budget assessment were necessary precondition to analyze the overall sea level budget, but also show the degree of reproducibility of the ocean mass variability time series by different algorithms and groups.

Relevant documents:

SLBC_cci Product Description Document D2.1.2:

> Novotny, K.; Horwath, M.; Cazenave, A.; Palanisamy, H.; Marzeion, B.; Paul, F.; Le Bris, R.; Döll, P.; Caceres, D.; Hogg, A.; Shepherd, A.; Forsberg, R.; Sørensen, L.; Andersen, O.B.; Johannessen, J.; Nilsen, J.E.; Gutknecht, B.D.; Merchant, Ch.J.; MacIntosh, C.R.: *ESA Climate Change Initiative (CCI) Sea Level Budget Closure (SLBC_cci). Product Description Document D2.1.2: Version 0 data sets and uncertainty assessments*. Version 1.2, 27 Sept 2017.

1.2 Document Structure

Chapter 2 discusses the global ocean mass budget as part of the global mean sea level (GMSL) change. Within this chapter, sources of ocean mass change (glaciers, ice sheets and hydrology) are compared to observed ocean mass changes. The subsequent Chapter 3 puts the GMSL into focus by looking at the mass and the steric component in GMSL change. The final Chapter 4 briefly discusses the budget of the Arctic Ocean. Auxiliary information on data used in Chapter 3 are given in the Annex.

1.3 Scientific Background

Sea level change, one of the best indicators of climate change, integrates the response of several components of the Earth system (ocean, atmosphere, cryosphere and hydrosphere) to anthropogenic and natural forcing. Studying the sea level budget helps to better understand processes at work and follow temporal changes (e.g., acceleration) of individual components. It increases our understanding on uncertainties of different observing systems and models. It also allows placing bounds on poorly known contributions (e.g., deep >2000 m ocean warming, not measured by current observing systems), constraining current Earth's energy imbalance and validating climate models used for simulating future climate. GMSL change as a function of time t is usually expressed by the sea level budget equation:

$$\Delta SL(t) = \Delta M_{ocean}(t) + \Delta SSL(t) \qquad \text{[Eq. 1]}$$

where $\Delta SL(t)$ refers to the change in sea level, $\Delta M_{ocean}(t)$ refers to the change in mass of the oceans and $\Delta SSL(t)$ refers to the steric contributions, namely the sum of ocean thermal expansion and the halosteric contribution, where in a global mean, the latter is due to global salinity conservation.

A major proportion of sea level change is due to the fact that water masses from land get re-distributed into the global ocean. The main sources are known to be melting glaciers and polar ice sheets, but also the variability in the onshore water masses budget has significant impact on sea level changes.

The ocean mass budget reads

$$\Delta M_{Ocean}(t) = - [\Delta M_{glaciers}(t) + \Delta M_{GIS}(t) + \Delta M_{AIS}(t) + \Delta M_{LWS}(t) + \text{other}], \qquad \text{[Eq. 2]}$$

where $\Delta M_{glaciers}(t)$, $\Delta M_{GIS}(t)$, $\Delta M_{AIS}(t)$ and $\Delta M_{LWS}(t)$ are the temporal changes in mass of glaciers, Greenland (GIS) / Antarctica (AIS) ice sheets and total land water storage (LWS), including seasonal snow cover. Other terms, e.g., atmospheric water vapour variability were only partly considered individually in the assessment. The mass budget misclosure, as used in this report, is

$$\text{misclosure} = \Delta M_{Ocean}(t) + [\Delta M_{glaciers}(t) + \Delta M_{GIS}(t) + \Delta M_{AIS}(t) + \Delta M_{LWS}(t)], \qquad \text{[Eq. 3]}$$

where the terms on the right-hand side in Eq. 3 now are the assessed mass changes of the respective components, including their errors.

This v0 report focusses on the comparison of trends, i.e. of long term changes of the components contributing to the sea level change. Closing the sea level budget therefore means, within the context of this study, evaluating linear trends of sea level and ocean mass changes.

Methodologies applied to calculate trends differ in Chapter 2, 3 and 4. The discussion on a common understanding about the methodologies and their differences is in progress within the SLBC_cci project but is not concluded yet.

A more detailed comparison of non-linear effects such as seasonal variations will be part of future work to be done within the SLBC_cci project.

Being a focus of the SLBC_cci project, the assessment of uncertainties of individual time series and combined products and trends is not trivial and demands an improved understanding of sources of uncertainty in the individual datasets and their relation to each other. With our approach in this project, we aim to reflect realistic uncertainties of the datasets assessed. While improved uncertainty assessments should ultimately trigger improvements in the product generation and hence *decrease* uncertainties, we expect that, in the first instance, improved uncertainty assessments may *increase* stated uncertainties. Comparisons of SLBC_cci results with previously published results, e.g. from the Dieng et al., 2017 study and the Chambers et al. 2017 study are valuable for evaluating our results. In Chapter 3 (see also Annex) we particularly refer to the Dieng et al. 2017 study, were we are able to compare the numerical results and to illuminate respective differences.

2 Ocean Mass Budget

2.1 Data update

For this chapter of the report, we used seven different GRACE-based solutions with observed mass changes over the global ocean. The products are partly taken from the SLBC_cci version 0 data pool as described in the Product Description Document D2.1.2 (see section 1.1). We also used ocean mass change time-series that have been improved over the version 0 products within the SLBC_cci project. The contributing terms of the named components on the right side of Equation 2 (see section 1.3) were entirely taken from the version 0 data pool as documented in D2.1.2.

“Other terms” according to Equation 2, e.g., atmospheric water vapor variability, were not considered individually in the assessment.

WP221 Ocean mass change from GRACE (see Figure 2.1). Ocean mass time-series from four solutions were used in a further improved version (called v0.2 and v0.3 thereafter). V0 data as described in D2.1.2 were improved in terms of processing after the global mass grid import; the underlying source data and correction models/coefficients remained identical:

- Mascon based solutions: CSR, JPL and GSFC globally integrated and scaled mass change time series. The three underlying, unchanged solutions as from D2.1.2 v0 were used. All three mascon processing centres provided their own dedicated land-ocean mask (CSR, JPL) or point-set (GSFC). Their differences reflect differences in the a-priori information for the masconprocessing. Different from D2.1.2, we have now (SLBC_cci OMC time-series version 0.3, WP222) used these product-specific land-ocean masks. We have adequately rescaled the obtained mass changes onto a common global ocean area of 3.61e+14 m². GSFC time-series were used with the provided OBP-indices (global ocean) excluding ice shelf indices.
- Spherical harmonics based solutions: ITSG (up to degree 60, as described in D2.1.2) time series and Chambers for CSR, GFZ, JPL (unchanged, as in D2.1.2) globally integrated and scaled time series. The mask applied to the ITSG data set was developed at TUDr and introduced with (internal) SLBC_cci version 0.2. It incorporates a 300 km leakage buffer around coastlines (and grounding lines) of landmasses larger than 20000 square kilometres. As compared to the mask used for ITSG v0 time series, it has buffer zones also around smaller islands (greater than 2000 square kilometres) in regions South of -49 degrees and North of 50 degrees, where otherwise leakage from land ice melt would occur. The maximum degree 60 and the 300km buffer width is motivated by the analysis by Johnson and Chambers (2013) and supported by own

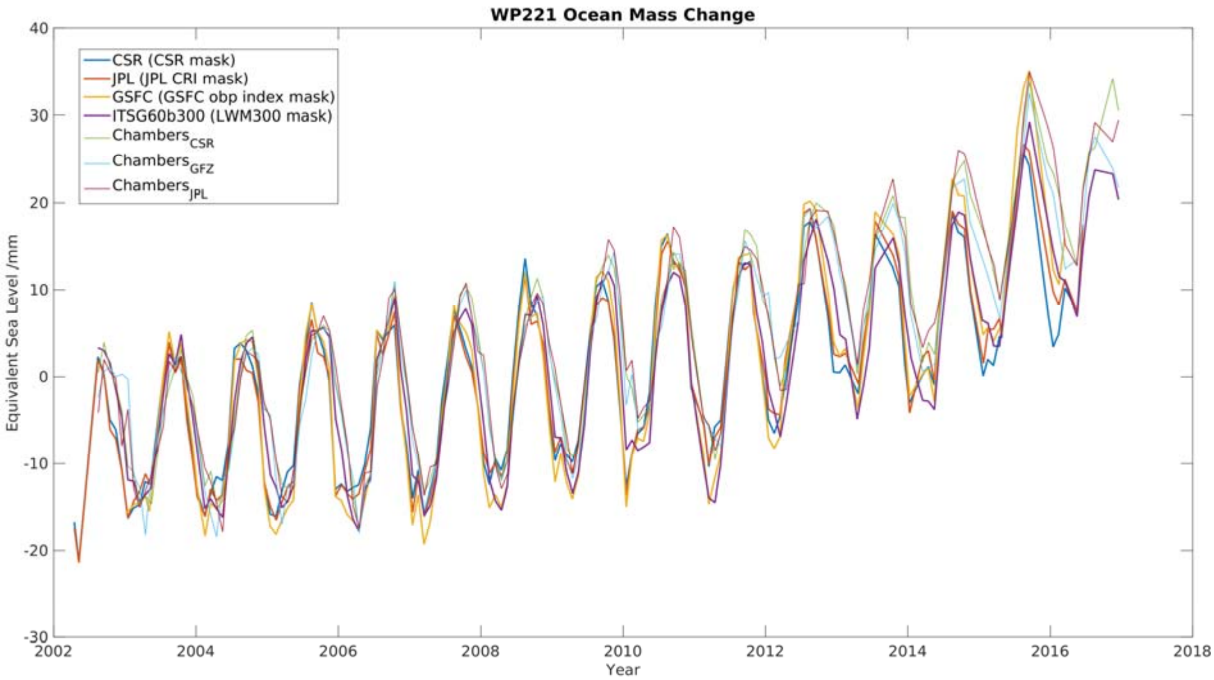

Figure 2.1: Ocean mass change from GRACE (WP221, 222) from SLBC_cci v0.3. Bold lines represent the three mascon-based solutions from CSR, JPL and GSFC and the solution based on spherical harmonic coefficients up to d/o 60 from ITSG. The three Chambers time series, based on the GRACE Science Data System solutions from CSR, GFZ and JPL, are shown as thin lines. All time-series still include strong seasonal signals. No smoothing or de-trending is applied.

Table 2.1: Uncertainties of the 300 km buffered ITSG60 GRACE-based ocean mass trends. Note that leakage errors and error correlations are not accounted for in this assessment.

Error source	Estimation procedure	Assessed standard uncertainty
Degree one	Intercomparison of different degree one time-series	0.138 mm/yr
C20	Intercomparison of different C20 time-series	0.219 mm/yr
GIA model	Intercomparison of different models	0.235 mm/yr
Combined uncertainty	Root sum square	0.350 mm/yr

investigations. Some details of their analysis, e.g. the choice of islandes considerdered for buffering. remain unknown to us.

The uncertainty assessments for GRACE-based ocean mass trends has been refined since D2.1.2, based on simulations with algorithms based on spherical-harmonic solutions, as operated at TU Dresden. The procedure is analogous to the assessment of trend uncertainties of GRACE-based AIS mass changes, as outlined in D2.1.2 (Section 5.3.5 therein). The preliminary uncertainty budget used for this report is shown in Table 2.1. An intercomparison of time series by Swenson et al. (2008, CSR-based), Rietbroek et al. (2016, inversion approach), Cheng et al. (2013a, SLR) and Bergmann-Wolf et al. (2014, ITSG-Grace2016 based) led to the Degree-one uncertainty estimation as given in Table 2.1. The C20 uncertainty estimation is based on Cheng et al. (2013b, SLR), Sun et al. (2016, GRACE and ocean model), Bruinsma et al. (2014, GRACE / SLR), Bloßfeld et al. (2015, SLR) and one additional C20 time series based on six SLR satellites, processed at GFZ Potsdam using the same background models and standards as applied during GFZ GRACE processing. The GIA models ICE-4 VM2 (Peltier, 1994), ICE-5G VM2 (A et al., 2013) and ICE-6G_C VM5a (Peltier et al., 2015) were used in order to assess GIA-related uncertainties in ocean mass.

The uncertainty assessment is not yet complete, as it does not include leakage errors. Moreover, error correlations between GRACE-based ocean mass change and GRACE-based ice sheet mass changes are not accounted for in this v0 assessment, even though they exist.

WP231 Glacier mass change (see Figure 2.2): Integrated mass change time series based on SLBC_cci v0 gridded data as documented in the Product Description Document D2.1.2. The given yearly time stamps were treated as mid-of-year (B. Marzeion, pers. comm.). Uncertainties were originally given as half width of the 90 percent confidence interval. To convert them to standard uncertainties (standard deviation of the error), here the numbers were divided by 1.645, based on the assumption of a normal distribution of the errors.

WP241 Ice sheets mass change (see Figure 2.3):

- GIS: GMB integrated mass change time series for entire Greenland (GIS00_grace.dat) as documented in the Product Description Document D2.1.2. Given time stamps at turn of the month were forward shifted to mid-of-month.

  Uncertainties of the trends were taken from Table 5 (bottom line) of D2.1.2. The expected range of accuracy errors of 9 Gt/yr given there translates into 0.025 mm/yr sea level. (Throughout this chapter we count 1 Gt land water or land ice to correspond to 1/361 mm equivalent sea level.) DTU-GDK assesses the total uncertainty to a larger value of 15.6 Gt/yr = 9 Gt/yr + 2*3.3 Gt/yr, where 9 Gt/yr arises from the accuracy assessment (Table 5 in D2.1.2) and 3.3 Gt/yr is the formal 1-sigma error of the linear fit to the time series. The internal discussion has not reached a conclusion as to whether and how the "total uncertainty" assessed by DTU-GDK can be considered as a quantification in the sense of a standard deviation or other parameters of a probability distribution of the total error. Therefore we cannot reach, at this stage, consistency between the approach of uncertainty quantification for GIS and the standard error approach attempted for the other contributions.

- AIS: GMB integrated mass change time series for entire Antarctica (AIS_GMB_basin.dat, AIS32) as documented in the Product Description Document D2.1.2. Uncertainties of the trends were taken from Table 6 of D2.1.2 (bottom line).

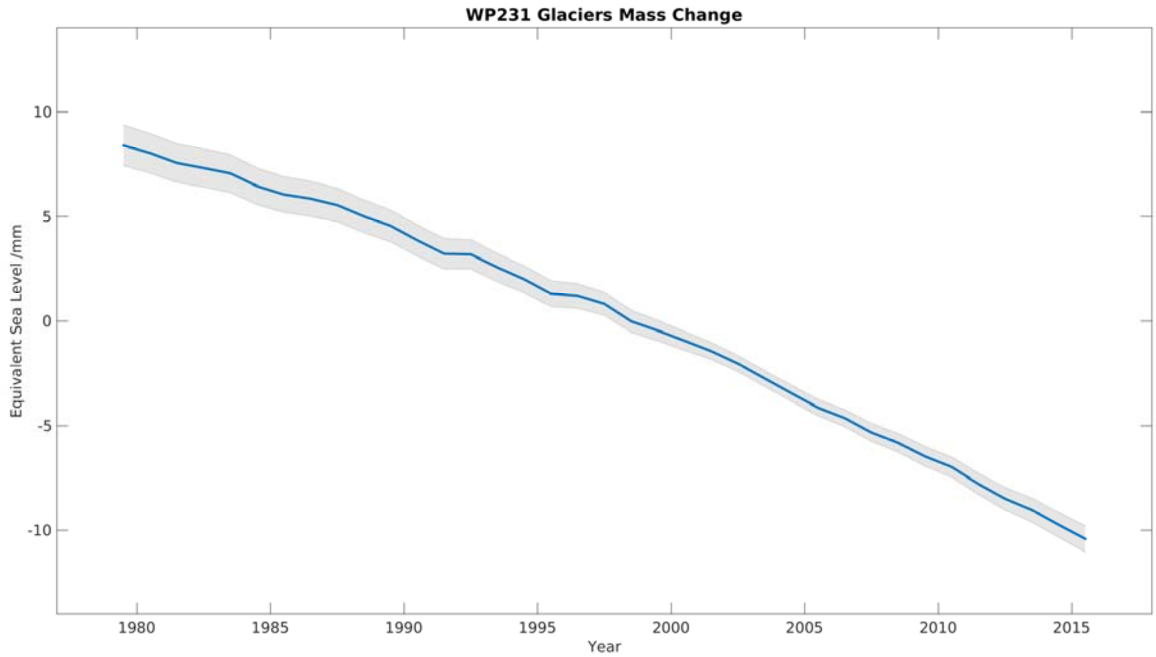

Figure 2.2: Glacier mass change in mm of equivalent sea level (WP231). Here, mass loss means gain for the global ocean. This SLBC_cci v0 data set has a time resolution of one year. No smoothing or de-trending is applied.

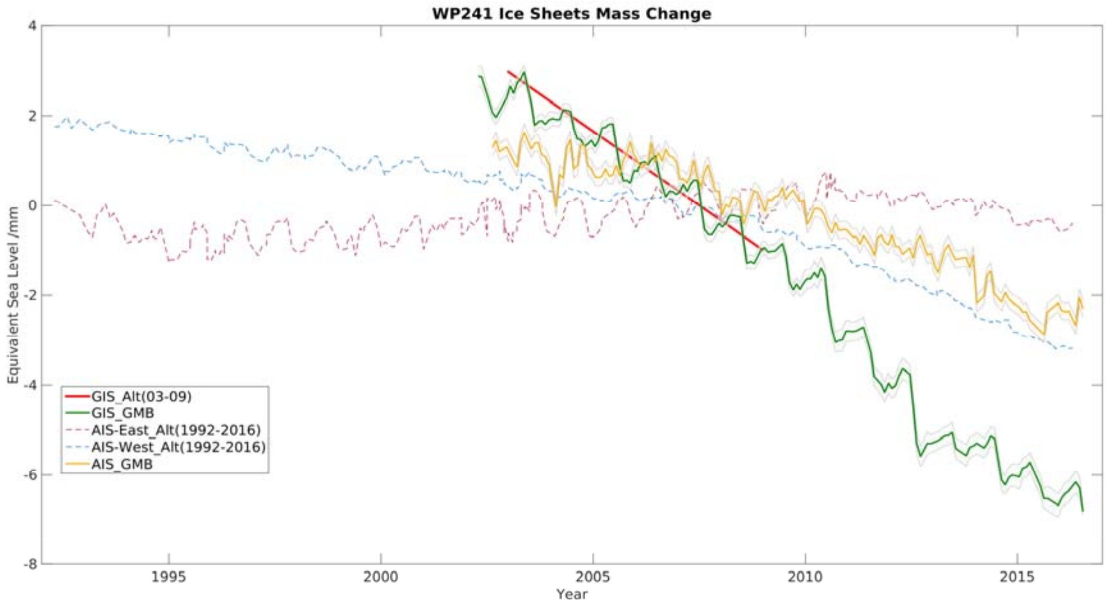

Figure 2.3: Mass change time-series for the Greenland (GIS) and Antarctic (AIS) ice sheets (WP241). Solid green and yellow curves with uncertainty ranges represent GRACE Mass Balance (GMB) products, which were used in this assessment. The bold red line represents an altimetry-derived trend for the GIS for the period 2003–2009. For all graphs, ice mass loss means ocean mass gain. No smoothing or de-trending is applied.

WP251 Land water mass change (see Figure 2.4): WFDEI-, CRU- and CRUGPCC driven globally integrated monthly time series of equivalent water heights (global_average_tws_without_greenland.xls) as documented in the Product Description Document D2.1.2, converted to mass and rescaled from source to ocean area. Given monthly time stamps were treated as mid-of-month (D. Cáceres, pers. comm.).

For the land water contribution, no uncertainty assessment is available. We did a preliminary uncertainty assessment based on the data. This is described in Section 2.2.1.

The following SLBC_cci version 0 available data have not been considered in this mass budget assessment:

- WP241 Ice sheets:
  - Altimetry based data of the Greenland ice sheet mass change were not considered in this assessment as it provides only one trend over a limited period of time. For the available shorter period of time, the altimetry based mass change estimate is in good agreement with the GMB derived mass change (see Figure 2.3).

- Altimetry based version 0 data for the Antarctic ice sheet mass change were not considered in this assessment as they represent change in mass in East- and West-Antarctica but not the Antarctic Peninsula, which is known to undergo a significant mass change.

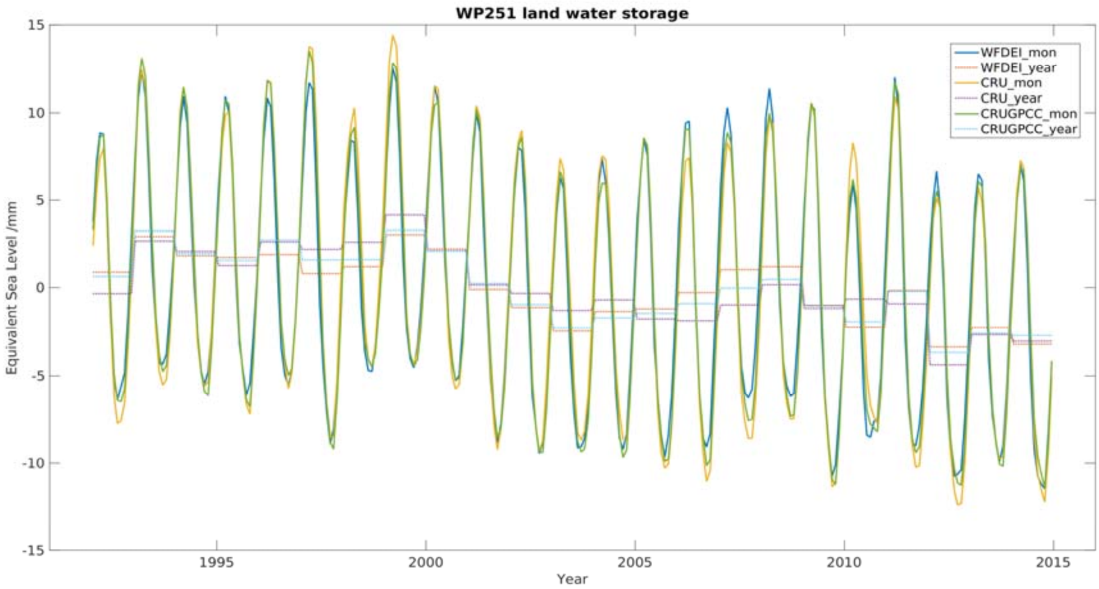

Figure 2.4: Total land water storage time-series of model forced with WFDEI, CRU and CRUGPCC input (WP251). Here, mass loss means gain for the global ocean. No smoothing or de-trending is applied. Note that these SLBC_cci v0 data sets end in December 2014. Yearly resolved LWS data (dotted lines) have not been used for this report.

2.2 Budget assessment

2.2.1 Methods

The time series of contributing components were limited to a common time interval from 01/2003 to 12/2014. The end time was defined by the used LSW time series, while all other time series extend at least to 12/2015. For the time series available through 12/2015 we repeated the analysis for the interval 01/2003–12/2015 for later reference. We additionally quote the results for this longer interval. Data that were not available as mass change time series but as grids per time, were globally integrated and scaled onto a common standard ocean surface area of 3.61e+14 m^2. Figure 2.5 summarizes the considered contributing components over 2003–2014.

An unweighted least squares fit of a 6-parameter function (consisting of a constant, a linear component, an annual cosine and sine function and a semi-annual cosine and sine function) was computed for each restricted mass change time series based on un-interpolated data, respectively. The linear component of this functional fit is treated as the trend. This trend is used for assessing the ocean mass budget.

Uncertainties of the trends are taken from D2.1.2 with the updates or conversions described in Section 2.1. They are considered as standard uncertainties (standard deviation of the error). Note that these uncertainties exceed the formal uncertainties of the functional fit because their assessment includes systematic effects (e.g. GIA uncertainty, in the case of GRACE-based data products). Uncertainties of sums or differences of the trends from individual contributions are taken as the root sum square of the individual uncertainties.

For a preliminary uncertainty assessment on the land water mass trends, we explored two approaches and finally used the approach that resulted in the largest uncertainty, while acknowledging that neither of the two approaches may represent the full uncertainty. The “ensemble spread approach” (cf. Müller Schmied et al. 2014) considers the spread between the linear trends obtained from the three land water mass time series, derived from three different atmospheric forcings. The “regression uncertainty approach” uses the formal error of the trend estimated from the 6-parameter functional fit to the mass change time series by considering autocorrelation of the residuals (e.g., Williams et al. 2003). We use statistics of the post-fit residuals, interpret them as statistics of the noise overlaid on the linear trend and propagate the noise statistics to the uncertainty of the trend. Standard procedures of this propagation assume serially uncorrelated noise. However, we found that the post-fit residuals are autocorrelated over about 12 months. Consequently, we scaled the formal error by sqrt(12)=3.464 to account for the fact that the number of independent samples for a trend estimate is about one twelfth of the number of monthly values. Note that the “correlated noise” considered here is largely a result of interannual variability and not a reflection of model errors.

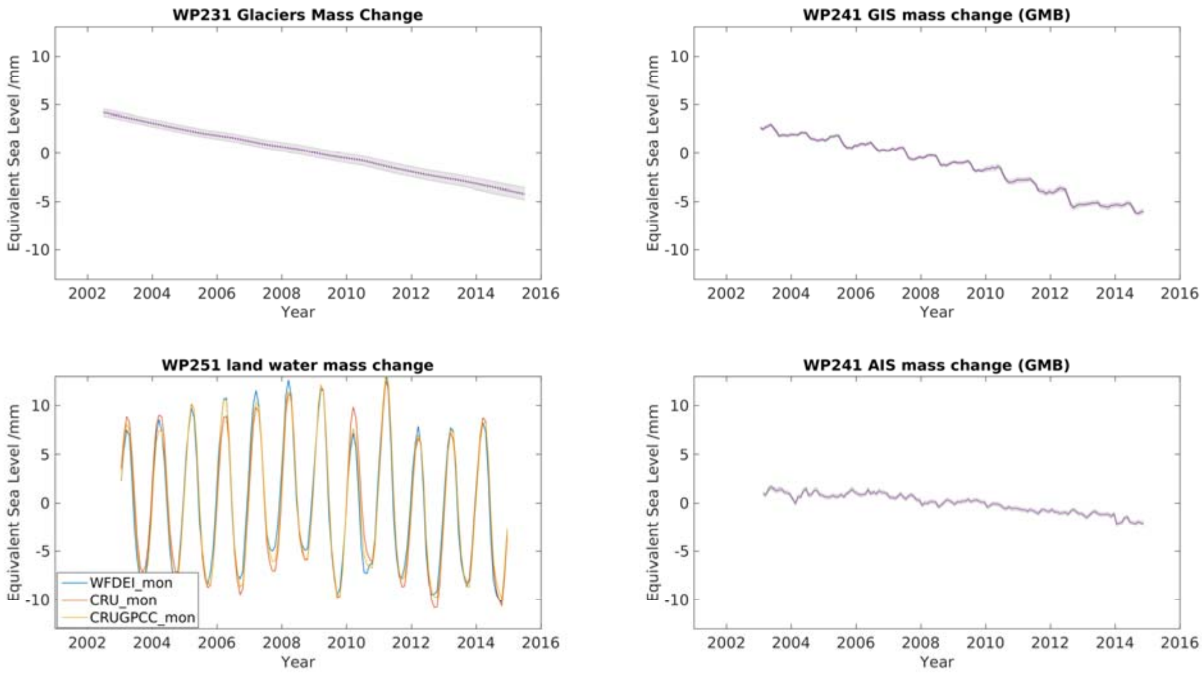

Figure 2.5: WP2x1 components applied to the ocean mass budget assessment (as in Figure 2.1 – Figure 2.4) plotted to the same scale and common time frame 2003–2014. No smoothing or de-trending is applied. Note the high seasonal amplitude in land water storage.

The mass budget was then derived from the linear components of (a) ocean mass change and (b) the sum of components, namely Glaciers, AIS, GIS and LWS (cf. Equation 2 and 3).

We generated two other sets of time series for purposes of displaying and of analyzing the non-linear and non-seasonal components.

- In one set of time series we reduced the annual and semi-annual components.
- In another set of time series we additionally reduced the linear component (trend).

In addition, we then interpolated those time series to a common mid-monthly temporal sampling. This interpolation was necessary for comparative analyses because of the inhomogeneous time basis of the underlying data products. Based on the common temporal sampling, we calculated the misclosure of the non-linear, non-seasonal components and analyzed it statistically. However, the trends considered throughout this assessment are solely based on original, un-interpolated time series.

2.2.2 Results for linear trends

The linear trends for all considered terms of the ocean mass budget are given in Table 2.2. For the time interval 2003–2014 (and 2003-2015, respectively), all considered components show a clear positive trend (with positive meaning mass loss on land):

- The sum of components is 1.81 +/-0.180 mm/yr for 2003–2014.
- The Greenland Ice Sheet has the largest contribution by 0.76(0.76) +/-0.025 mm/yr.
- The glaciers contribute with 0.63(0.63) +/-0.033(0.031) mm/yr.
- The combined Antarctic Ice Sheet's contribution is 0.27(0.29) +/-0.098 mm/yr.
- The trend in land water storage for three provided model variants ranges from 0.11 mm/yr to 0.18 mm/yr. The ensemble mean is 0.15 mm/yr, which is about the same as the trend with WFDEI forcing. A LWS ensemble mean is applied for the subsequent budget assessment. The uncertainty of the LWS trend is 0.03 mm/yr based on the "ensemble spread approach" and 0.145 mm/yr based on the "regression uncertainty approach" (see Section 2.2.1). We use the larger uncertainty from the "regression uncertainty approach" for the following assessment. We acknowledge the wide spread of the two uncertainty estimates (cf. also the 0.09 mm/yr estimate by Dieng et al. 2017 - see Table 3.1). It highlights the need for further investigations on realistic and consistent uncertainty estimates.

SLBC_cci version 0 data of total LWS is only available until December 2014, which lets us only produce valid estimations for 2003–2014. In order to make use of other component data that are available until end of 2015, we used the same LWS trend also for a comparison with trends of data available until 2015. However, this might introduce errors of uncertain magnitude.

The misclosure of the trend for the common period 2003–2014 is -0.15 mm/yr when an ensemble mean of all seven GRACE-based solutions is considered. The spread between the misclosures resulting from the seven different GRACE OMC series has a standard deviation of 0.238 mm/yr.

Details about the dependence of the misclosure from the used GRACE OMC dataset are given in Table 2.3. A LWS ensemble mean was applied throughout this analysis. While the trends of mascon- and ITSG-based solutions all have lower trends than the sum of components, all trends for time-series by Chambers are larger than the sum of components. The smallest single mass budget misclosure for the OMC trend in the period 2003–2014 can be found for Chambers_GFZ (+0.05 mm/yr) and Chambers_CSR (+0.07 mm/yr). Systematically negative misclosures in the order of -0.3 to -0.4 mm/yr were found for CSR (mascon) and ITSG.

Table 2.2: fitted trends, their standard uncertainties, and misclosure for the period 2003-2014 (2003-2015)

	Trend 2003-2014 mm/yr	Uncertainty 2003–2014 mm/yr	Trend 2003-2015 mm/yr	Uncertainty 2003–2015 mm/yr
COMPONENTS:				
Glaciers	0.627	+/- 0.033	0.631	+/- 0.031
GIS (GMB)	0.760	+/- 0.025	0.756	+/- 0.025
AIS (GMB)	0.272	+/- 0.098	0.287	+/- 0.098
LWS ensemble {WFDEI / CRU / CRUGPCC}	0.147 {0.151 / 0.178 / 0.112}	+/-0.145	0.147* *) LWS is restricted to end of 2014 in SLBC_cci version 0; use trend 2003-2014 here	+/-0.145*
Sum of components	**1.805**	**+/- 0.180**	**1.821**	**+/- 0.180**
OMC (SLBC_cci v0.3):				
1) CSR mascons CSR-mask	1.401		1.495	
2) JPL mascons JPL-mask	1.574		1.687	
3) GSFC mascons with GSFC obp index mask	1.595		1.813	
4) ITSG SH60 b300km with LWM300 mask	1.338	+/-0.350 (+/- leakage & other)	1.506	+/-0.350 (+/- leakage & other)
5,6,7) Chambers {CSR / GFZ / JPL}	1.886 {1.872 / 1.851 / 1.935}		2.035 {2.030 / 1.983 / 2.092}	
Ocean mass change trend mean of 7 solutions	**1.652**		**1.801**	
Misclosure	**-0.153**	**Combined uncertainty from sum of components and OMC: Sqrt($0.180^2 + 0.350^2$) = 0.393**	**-0.020**	**Combined uncertainty from sum of components and OMC: Sqrt($0.180^2 + 0.350^2$) = 0.393**

Table 2.3: trend misclosure between OMC solutions and sum-of-components for 2003–2014 and 2003–2015.

mm/yr	1: CSR_m	2: JPL_m	3: $GSFC_m$	4: $ITSG_{60b300}$	5: $Cham_{CSR}$	6: $Cham_{GFZ}$	7: $Cham_{JPL}$	mean of 1–7
Misclosure 2003–2014 [STD of misclosure]	-0.404	-0.231	-0.210	-0.467	+0.067	+0.046	+0.130	-0.153 [+/-0.238]
Misclosure 2003–2015 [STD of misclosure]	-0.325	-0.133	-0.008	-0.314	+0.210	+0.163	+0.271	-0.020 [+/-0.246]

2.2.3 Results for time series with full temporal resolution

Figure 2.6 shows the comparison between the individual components, the sum of components, and the OMC on a monthly time series basis. In this figure, results are displayed for the ensemble mean of the GRACE OMC series and the ensemble mean of the three LWS model runs.

Figure 2.7 shows the misclosure time series for every individual GRACE OMC time series and for their ensemble mean. (The LWS time series is fixed to the LWS ensemble mean for this figure). The different trends in the misclosure that arise for different GRACE OMC series are obvious. In addition, differences also occur for the nonlinear components of the misclosure.

Figure 2.9 shows the misclosure for the individual LWS time series (where now the GRACE OMC time series is fixed to the OMC ensemble mean). The choice of the LWS model run appears to have a minor impact on the misclosure time series.

In addition to looking at the misclosure in terms of linear trends, we further analyze the misclosure on a time series level statistically.

Table 2.4 shows the standard deviations of the monthly resolution time series of misclosure for the different GRACE-based ocean mass change products. The statistics are shown for (a) the full time series, (b) the time series after removal of the seasonal signal (from the annual and semi-annual sinusoidal fit), and (c) after removal of the seasonal signal and the linear trend.

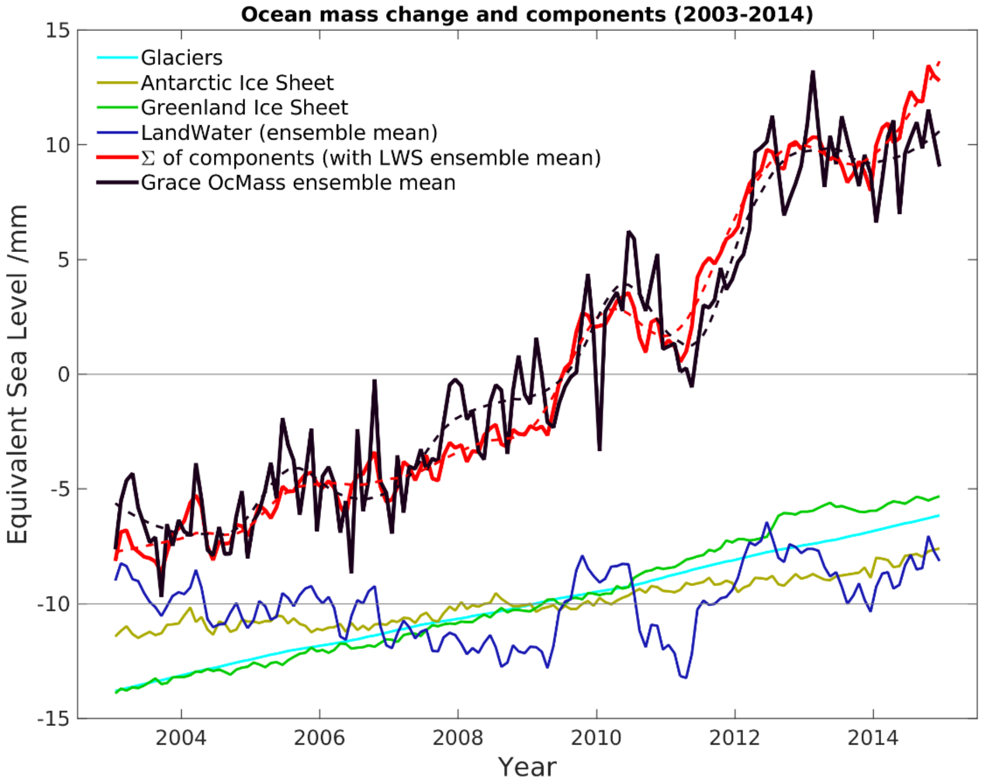

Figure 2.6: Time series of individual components, sum of components (bold red, with LWS ensemble mean) and OMC (bold black, ensemble mean). For reasons of clarity the contributing components were shifted by -10 mm e.s.l. Seasonal signal is removed from each time series, interpolation to common time sampling (mid-of-month) was performed. Dashed lines: smoothed, for visualization only.

The STD of the misclosure decreases significantly (from 3.23 mm e.s.l. to 2.24 mm e.s.l.) after removal of the seasonal components. This points to a misclosure of the seasonal components, which may be the subject of future investigations.

The STD of the misclosure decreases further after removal of the linear trends. This is expected due to the misclosure of the linear trends themselves, as shown in Table 2.3.

The STD of the misclosure in the non-linear and non-seasonal components (last line in Table 2.4) indicates that Chambers_CSR and ITSG60b300 show the smallest mass budget misclosure for those temporal components. More details on the statistics of the misclosure of the non-linear, non-seasonal components are shown in Figure 2.8.

Further analyses will be needed to clarify to what degree the differences in the misclosure STD are affected by different month-to-month noise content and by different representations of interannual signal.

Table 2.4: standard deviations of the monthly resolution time-series misclosure (2003–2014) for the different OMC solutions a) with included seasonal and linear components, b) after reduction of the seasonal signals and c) after additional reduction of the linear component.

STD of monthly misclosure /mm	1: $CSR_{mascons}$	2: $JPL_{mascons}$	3: $GSFC_{mascons}$	4: $ITSG_{60b300}$	5: $Cham_{CSR}$	6: $Cham_{GFZ}$	7: $Cham_{JPL}$	mean (1–7)
(a) Incl. seasonal and linear	3.84	3.51	3.91	2.84	2.68	2.87	2.95	3.23 +/- 0.51
(b) Non-seasonal	2.63	2.55	2.58	2.30	1.62	2.08	1.94	2.24 +/- 0.38
(c) Non-seasonal and non-linear	2.23	2.43	2.49	1.65	1.61	2.09	1.89	2.05 +/- 0.35

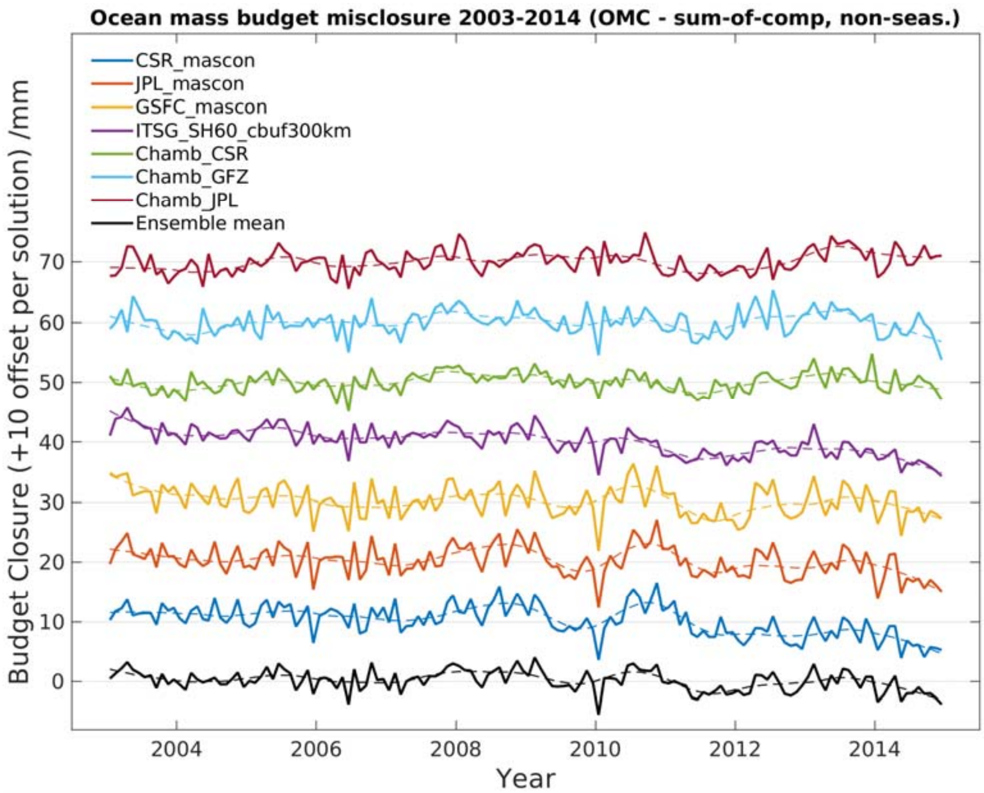

Figure 2.7: Time series of the ocean mass budget misclosure based on the seven OMC solutions, respectively. In addition, the misclosure for the OMC ensemble mean, as given in Figure 2.6, is shown in black. Seasonal signals are removed. Dashed curves smoothed time series, for visualization only.

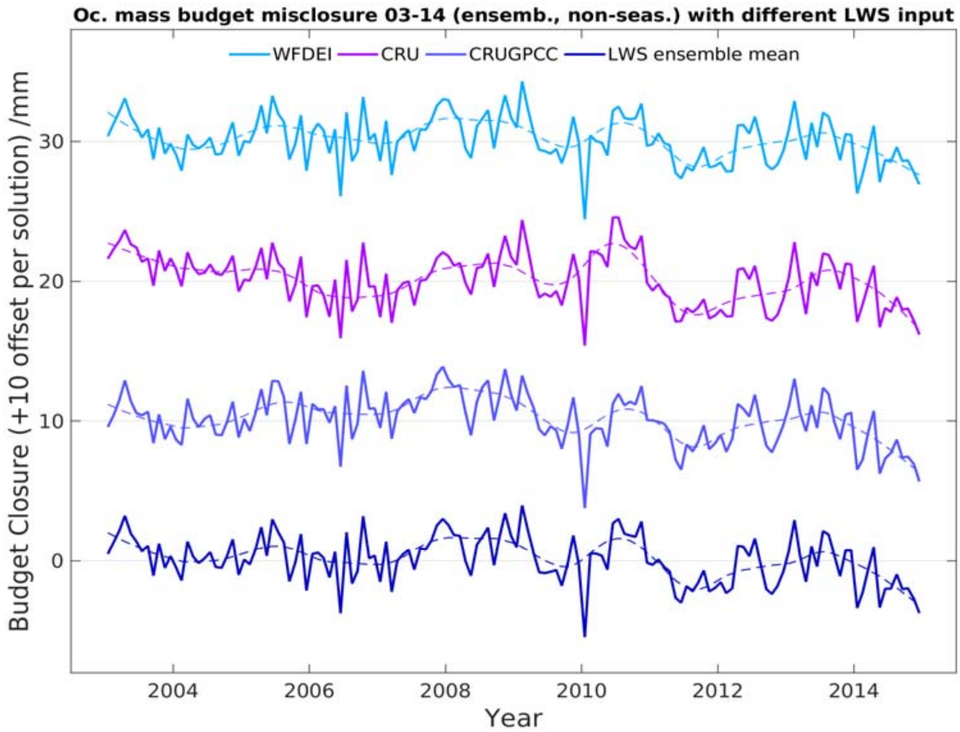

Figure 2.9: Ocean mass budget misclosure with three different forcings of the LWS model and the ensemble mean of the three LWS models. The OMC time series ensemble mean is used here. Seasonal signals are removed. (dashed curves: smoothed, for visualization only)

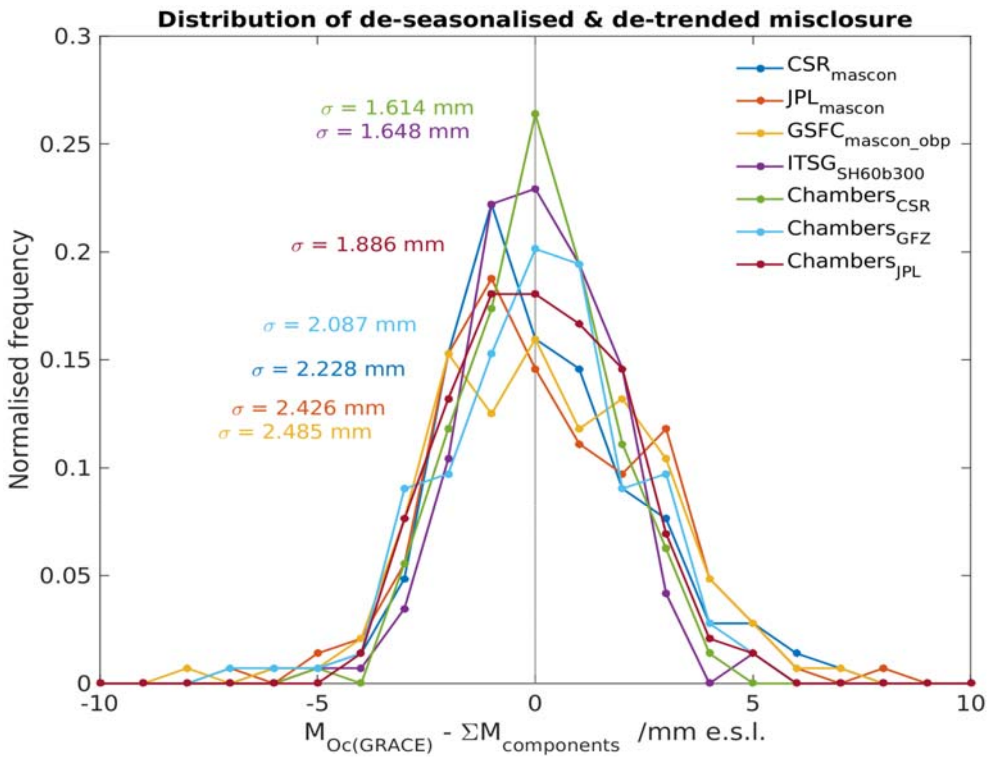

Figure 2.8: Histograms of monthly misclosure between the seven mid-monthly interpolated OMC time-series and sum-of-components after reduction of seasonal signals and the linear trend.

2.3 Discussion

The misclosure of the linear trends over 2003-2014 is within the combined uncertainty of OMC and the sum of components. Hence, the ocean mass budget in terms of linear trends is closed within its uncertainty.

It is worth noting that the GIA correction, the Degree-1 series, and the C20 series are chosen identical (according to documentations) for all GRACE-based OMC estimates used here. Therefore, even though GIA, Degree-1, and C20 constitute large sources of *uncertainty*, the *errors* from these three elements should be approximately the same in all GRACE-based OMC series. Therefore such errors are not likely to explain the considerable spread between GRACE-based OMC results. This spread needs to be further investigated in the future.

Time series including seasonal cycles show a considerably larger mismatch between the observed signal and the sum of contributing components. Time series from which the seasonal cycle has been removed show a considerably better budget closure.

The assessment of trend uncertainties of the considered mass change components of land, cryosphere and ocean differ considerably. While the glacier and ice sheet mass change trend uncertainties are relatively well known in order to be considered, an equivalent for the trend in changes of land water masses is still to be determined. However, GRACE-based ocean mass time series show significantly larger (at least twice of components) uncertainties and are partly unknown for several solutions.

Signal leakage into the ocean from mass changes that occur on land has been considered in the latest SLBC_cci v0.2/0.3 updates by application of dedicated land-ocean masks but may continue to persist with different magnitude for the different solutions, respectively, and is not well known at this point. Furthermore, masking out leakage-prone ocean areas may lead to omission of actual ocean mass loss signals near ice-loss areas on land (fingerprint).

3 Global Sea Level Budget

In this section we discuss the results of the global mean sea level budget closure analysis.

Note that the GRACE OMC products used in this section differ from the respective GRACE OMC products used in Section 2, for reasons explained in Section 3.1

3.1 Data update

For this first report, we focus on the 2003-2015 period because the version 0 of some components (Greenland and Antarctica ice sheets) were not yet available for the 1993-2003 time span at the time of analysis. We expect that the forthcoming versions 1 of these products will cover the whole altimetry period.

The 2003-2015 budget is analyzed below using 2 approaches:

1. Use of individual mass components for the ocean mass contribution (according to Equation 2, Section 1.3),
2. use of GRACE-based ocean mass estimates.

For approach 1, we used the v0 products provided by the partners of the project.

For approach 2, we used the original v0 time series provided by TU Dresden as delivered in D2.1.1 and described in the Product Description Document D2.1.2. Although the landmasks used for the v0 products were later updated to produce v0.2/v0.3 OMC products, these updated products were not available from TU Dresden before the internal deadline for this analysis. Therefore, no respective update of used OMC products for the sea level budget was possible.

3.2 Analysis of individual sea level component

In this section, we analyze the sea level budget using the SLBC_cci version 0 for the individual mass components. We also compare these with those from external sources such as the recent publication by Dieng et al., 2017 (see annex for a description of the data sets used in Dieng et al., 2017).

The v0 products used here are described below. For all data sets, we removed the annual and semi-annual cycles through a least-squares fit of 12-month and 6-month period sinusoids. No interpolation was performed to fill any existing data gaps in the time series. Linear trends were then estimated using the least squares fit methodology on the un-interpolated data without annual and semi-annual cycles.

For the products whose mass components and associated errors are provided in gigatons (Gt) per year, we converted them into mm of sea level equivalent (SLE) by dividing by a factor of 360 (taking into account that 360 Gt of ice mass would raise globally the mean sea level by 1 mm approximately). All results below are expressed in mm SLE.

Any other specific data processing performed for each of the cases is explained under the corresponding section.

3.2.1 Mass components of sea level change

3.2.1.1 Glaciers

The global glacier mass change is obtained by summing over all the regions of interest. Uncertainty is obtained by taking the square root of the sum of the squares of the uncertainties over all the regions of interest as suggested in the Product Description Document D2.1.2. No other specific data processing was performed on the SLBC_cci_v0 glacier data.

Figure 3.1 shows the comparison between the SLBC_cci_v0 glacier mass time series in terms of SLE with the corresponding time series from Dieng et al., 2017. The SLBC_cci trend value for the 1993-2015 period amounts to 0.63 ± 0.04 mm/yr (Table 3.1).

The two time series and uncertainties shown in Figure 3.1 differ because Dieng et al. 2017 use the ensemble mean of three studies (Leclercq et al. 2011, Cogley et al. 2009, and Marzeion et al. 2015) together with the ensemble spread, wile SLBC_cci is based on Marzeion et al. 2015 together with its own stochastic error characterisation.

3.2.1.2 Ice sheets mass balance

Greenland

For the Greenland ice sheet mass balance time series, we used the GRACE-based SLBC_cci_v0 time series between 2003 and 2015. Figure 3.2 shows the comparison between the SLBC_cci_v0 Greenland ice sheet mass time series with the corresponding time series from Dieng et al., 2017. The SLBC_cci_v0 trend value for the 2003-2015 period amounts to 0.76±0.025 mm/yr (Table 3.1). The uncertainty is based on the error range provided in the SLBC_cci_v0 Product Description Document D2.1.2 (Table 5). Altimetry based Greenland ice sheet mass change data provided by WP241 has not been used in the study as the data covers only 2003-2009.

Antarctica

Two sets of Antarctica mass balance data were available from the SLBC_cci_v0: Altimetry-based mass changes from March 1992 to March 2016 and GRACE-based mass change data from 2003. However in this study, we considered only the GRACE based mass change data from 2003 as the altimetry based data represent only the East and West Antarctica mass change but not the Antarctic Peninsula, thus not the whole Antarctica mass balance. Moreover, the data set also has a time stamp issue that hinders its usage. Over 2003-2015, the trend value corresponds to 0.29±0.1 mm/yr for GRACE-based SLBC_cci_v0 Antarctica contribution (Figure 3.3, Table 3.1).

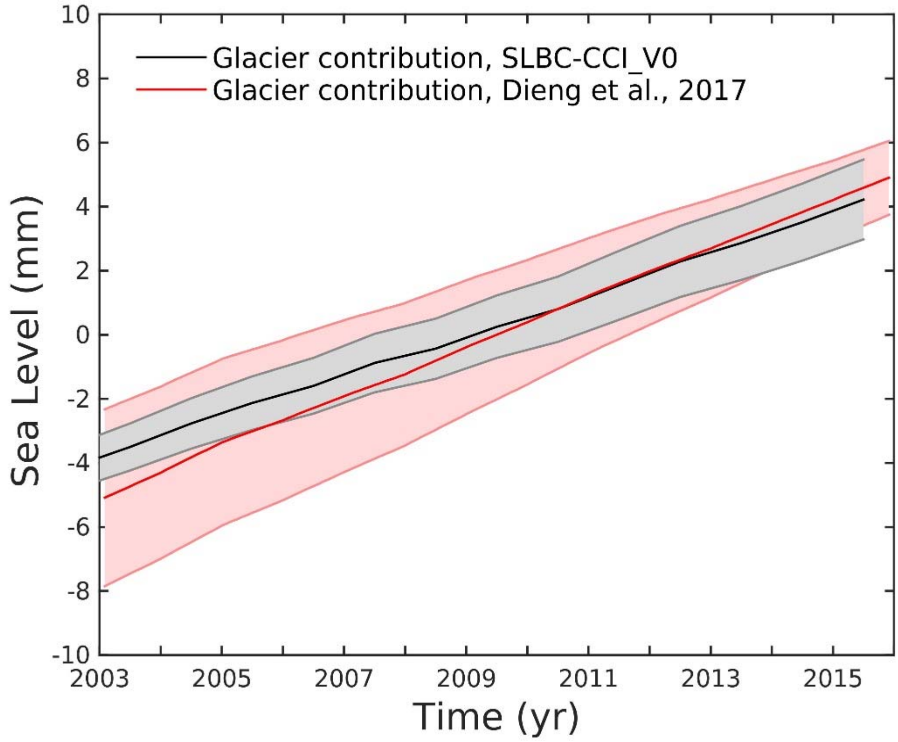

Figure 3.1: Global mean glacier mass change time series in terms of equivalent sea level (mm).

Table 3.1: Trend of individual components used in the sea level budget analysis over 2003-2015

	2003-2015 Trend (mm/yr)	
	Dieng et al., 2017	**SLBC_cci_v0**
Glacier	0.77±0.08	0.63±0.04
Greenland	0.8± 0.05	0.76±0.03
Antarctica	0.32±0.06	0.29±0.10
Total Water Storage	0.23±0.09	0.17 (until 2014)
Water Vapor	-0.07	-0.07
Steric	1.14±0.09	1.14±0.09

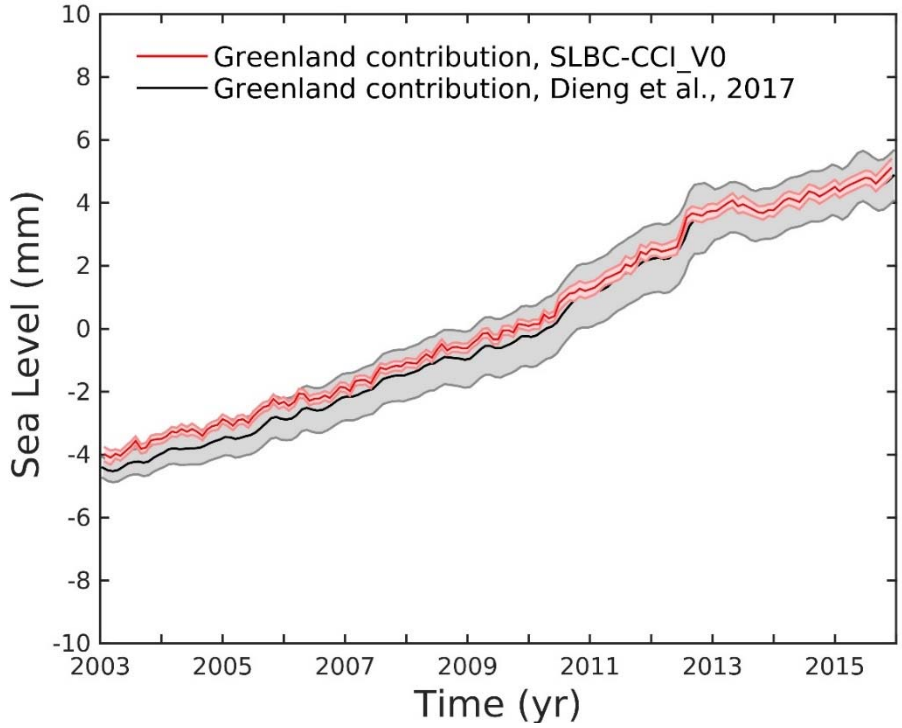

Figure 3.2: Greenland ice sheet mass change in mm SLE.

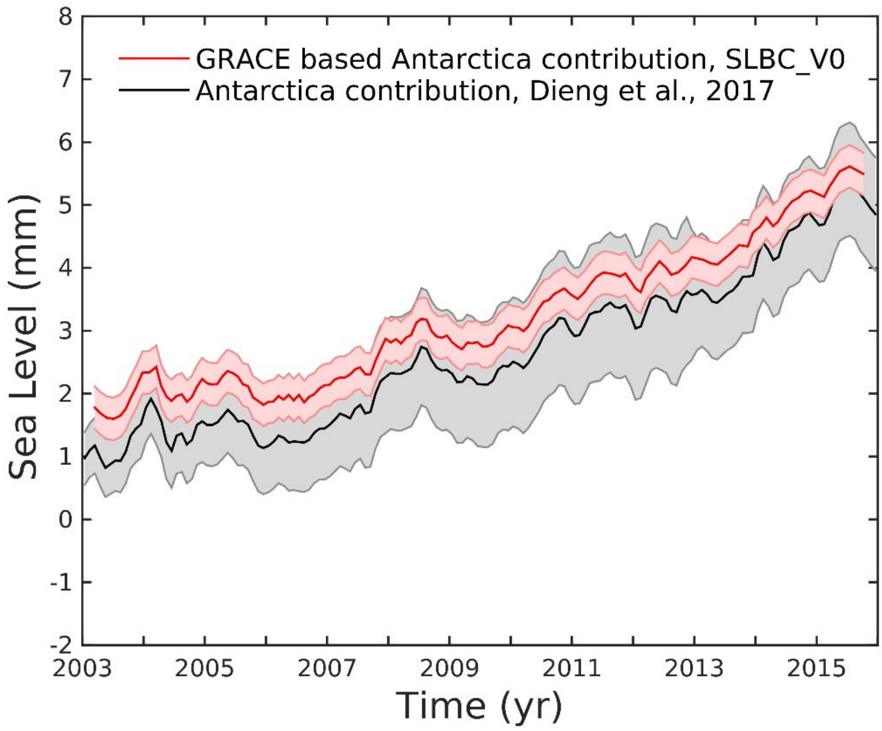

Figure 3.3: Antarctica mass change in terms of mm SLE between 2003 and 2015. For clarity, an arbitrary offset has been added to the red curve.

3.2.1.3 Total land water storage

Three different versions of the WaterGAP hydrological model (WGHM) based on different climate forcings are available from SLBC_cci_v0. From these, total water storage (TWS) time series corresponding to WFDEI (Watch Forcing Data based on ERA-Interim reanalysis) climate forcing based on Döll et al., 2014a,b was considered for the budget analysis. This version was used following the suggestion of the land water partner of the SLBC_cci project. Figure 3.4 shows the TWS contribution to sea level for the WFDEI SLBC_cci_v0 and Dieng et al., 2017 data sets. A 3-month smoothing was applied to the time series. We can observe that the two TWS products agree very well in terms of trend and interannual variability. Over 2003-2014, the WFDEI SLBC_cci_v0 trend accounts to 0.17 mm/yr (no uncertainty provided; Table 3.1). It has to be noted that the version 0 TWS time series extend only until 2014 while the other sea level components extend until 2015. In order to be consistent, the TWS trend value corresponding to 2003-2014 was used for the sea level budget analysis over 2003-2015. We are however aware that this will further increase the uncertainty range of the budget.

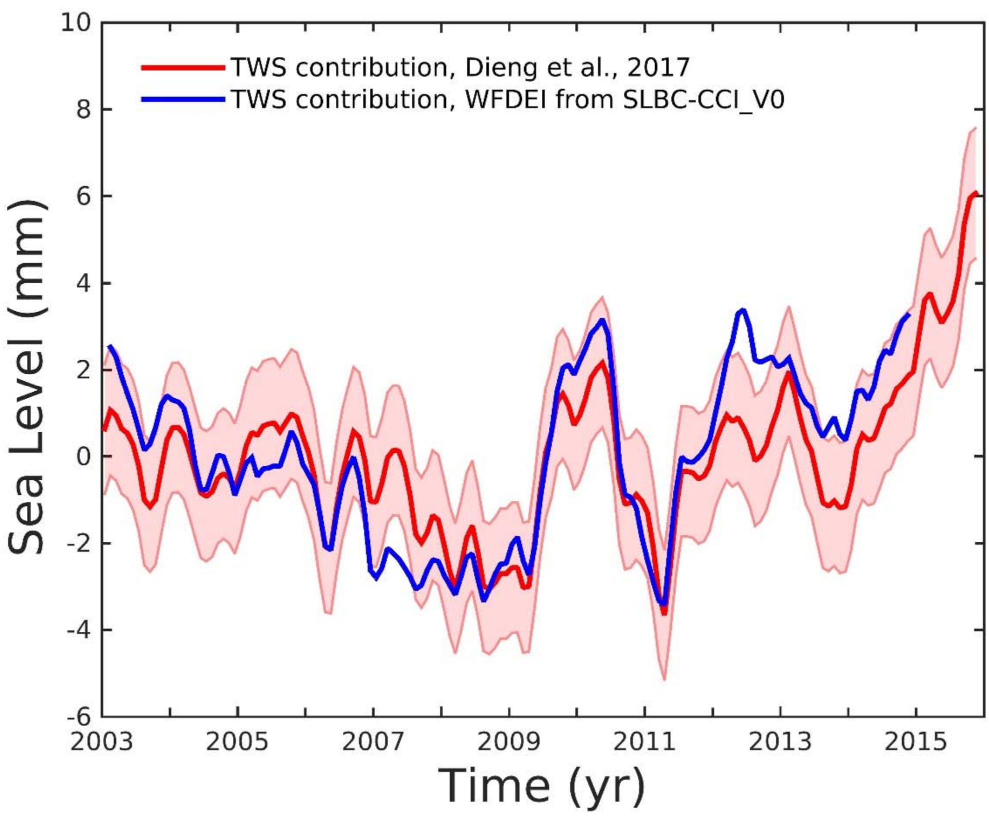

Figure 3.4: Total land water storage change in mm SLE between 2003 and 2014.

3.2.1.4 Total water vapor

To estimate changes in atmospheric water vapor mass, we used the ERA Interim reanalysis from ECMWF (European Centre for Medium-range Weather Forecast), as used in Dieng et al., 2017. Figure 3.5 displays the atmospheric water vapor contribution in mm SLE. The trend over the period of interest 2003-2015 amounts to -0.07 mm/yr (Table 3.1). The contribution of total water vapor to GMSL remains small and currently we are not aware of the impact of uncertainties due to the reanalysis data on this component. In future budget analysis, actions will be taken to obtain total atmospheric water vapor with its corresponding uncertainty range. If not possible, its contribution to GMSL will be considered as one of the uncertainty components.

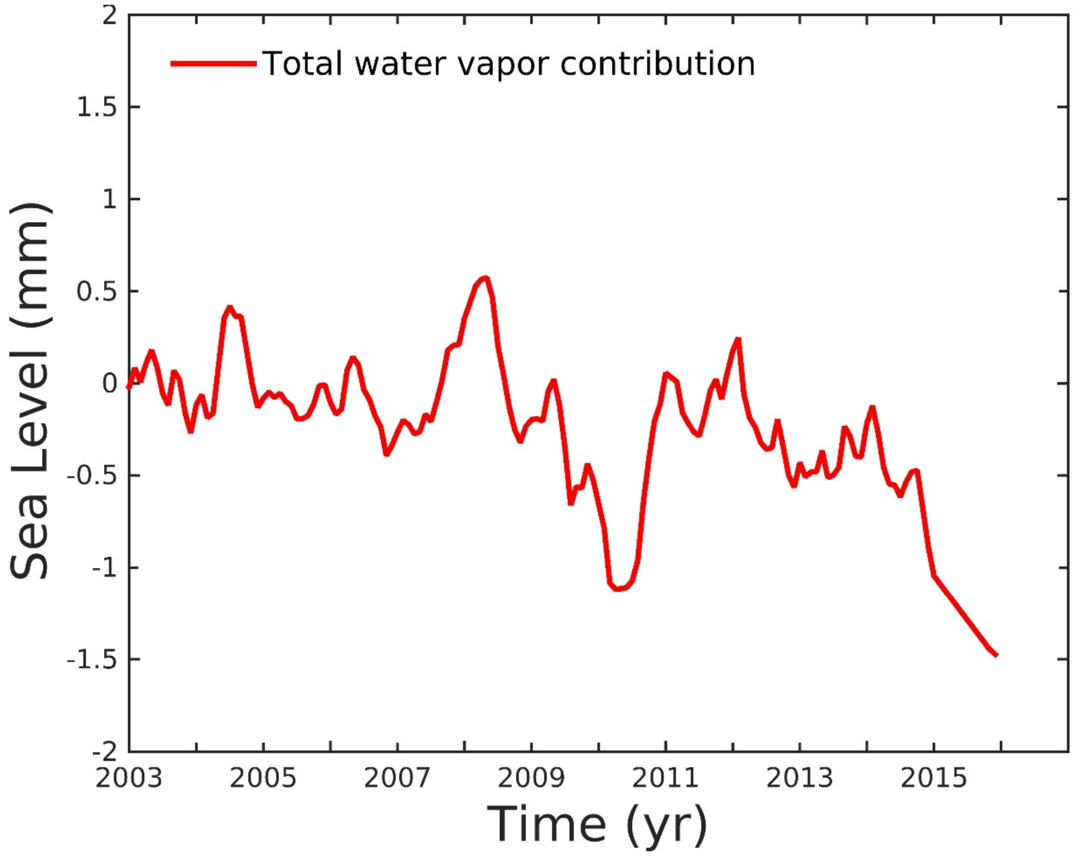

Figure 3.5: Total water vapor mass from ERA-Interim (in mm SLE) between 2003 and 2014.

3.2.2 Steric sea level

The SLBC_cci_v0 steric sea level data from LEGOS is the same as that used in Dieng et al., 2017 (see Annex of this report). Trends are given in Table 3.1.

The version 0 of the SLBC_cci project also provides steric data from the University of Reading based on von Schuckmann and Le Traon, 2011. However, this is not considered at this step as the data covers only the time period of 2005-2012 (see Figure 3.6). Furthermore, an updated version of von Schuckmann and Le Traon, 2011 steric data has already been considered in the ensemble mean from Dieng et al., 2017. Dieng et al., 2017 estimated the steric sea level uncertainty over each time step and for linear trend following the methodology mentioned in the Annex. The future SLBC_cci steric sea level versions will be provided with a dedicated uncertainty estimate as proposed by the WP210 partners (see Annex).

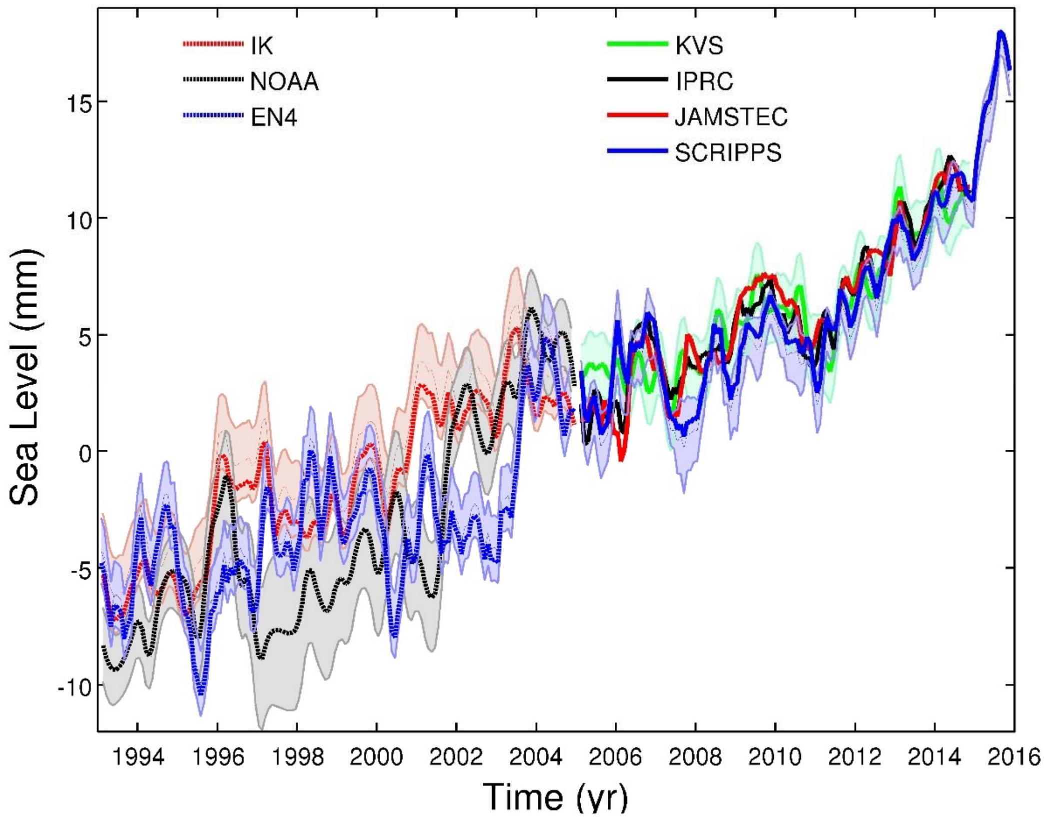

Figure 3.6: Steric sea level time series from XBT and Argo as in Dieng et al., 2017. Datasets are summarized in the summary. Abbreviations in the legend are explained in the list of acronyms and abbreviations (p.9)

3.2.3 Altimetry based sea level data

We used the version 2.0 (v2.0) of the GMSL time series provided by the ESA CCI sea level project (Ablain et al., 2017, Legeais et al., 2017). Uncertainty at each time step is not provided for ESA CCI GMSL time series (or for any other GMSL time series). Therefore for the CCI GMSL time series, uncertainty at each time step is estimated based on random dispersion of 6 available observed GMSL products (see Annex) around the ensemble mean as in Dieng et al., 2017. GMSL trend uncertainty used in this study is from Ablain et al., 2017 where the authors take into account uncertainty due to instrumental errors and geophysical corrections.

3.2.4 Comparison of the v0 mass components with those of Dieng et al., (2017)

In Table 3.1, we compare the trends estimated for the v0 components with those of Dieng et al., 2017. As noted above, the water vapor and steric contributions are from Dieng et al., 2017 in the absence of other available products in the preliminary analysis.

The two sets of trend data agree within their respective uncertainties, except for the glaciers which show a difference beyond stated uncertainties.

3.3 Intercomparison of SLBC_cci v0 GRACE ocean mass solutions with external GRACE solutions

As already mentioned in Section 3.1, this section uses the original v0 GRACE ocean mass data (compared with slightly improved versions v0.2/v0.3 used in Chapter 2).

The comparison of version 0 of the SLBC_cci ocean mass data was performed using the following data sets:

Global ocean mass time series processed as a part of the SLBC_cci project:

- CSR Mascons
- JPL Mascons
- GSFC Mascons
- ITSG, spherical harmonics (d/o 60) based ocean mass product with 300 km coastal buffer.

These were compared with the GRACE ocean mass products processed by D. Chambers using the spherical harmonics solutions (d/o 60) from CSR, GFZ and JPL (update from Chambers and Bonin, 2012; details given in Dieng et al., 2015). Furthermore, recently we also compared the CSR, JPL and GSFC mascon solutions processed by SLBC_cci_v0 with the same datasets downloaded and processed at LEGOS. This gives us a direct comparison (mascon to mascon comparison) and therefore an estimate of the differences in terms of trends that could rise from data processing (e.g. choice of ocean mask, coverage, etc.). Just as the GRACE ocean mass products used in Section 2, all GRACE ocean mass products used in Section 3 are corrected for Glacial Isostatic Adjustment (GIA) based on the GIA model of A et al., 2013.

A 3-month smoothing was applied to LEGOS GRACE mascon data when preparing the figures for a better appearance.

A preliminary analysis of the SLBC_cci_v0 CSR mascon solution indicated much lower trend than the other solutions. Based on discussions with the TU Dresden partner (M. Horwath and co-workers), it appeared that this arises from problems in the land-ocean mask used for that solution. It was therefore decided to not consider at the moment the CSR mascon solution for the v0 assessment. The comparison between the various SLBC_cci_v0 GRACE and LEGOS GRACE products is shown in Figure 3.7. **Table 3.2** summarizes the trend values between 2003 and 2015. The SLBC_cci CSR time series is plotted in Figure 3.7 only for comparison purpose, but not considered for the budget assessment.

Figure 3.7 shows that as of mid-2011, the GRACE ocean mass trend increases significantly for all solutions compared to the 2003-2011 time span. As summarized in **Table 3.2**, GRACE ocean mass trends are significantly smaller over 2003-2011 than over 2003-2015 (due to larger trends beyond 2011). Significant data gaps affect the GRACE data since 2012 because of instrumental ageing problems. But it is unclear how these gaps affect the GRACE ocean mass time series. More investigations on this will be carried out in the future. From **Table 3.2**, we note slightly higher trend values for the mascon solutions processed at LEGOS compared to SLBC_cci_v0, but similar relative trend differences for the two time spans (2003-2011 and 2003-2015). The Chambers solutions systematically give higher trends.

In terms of interannual variability, we find that all GRACE products (all mascon and Chambers solutions) agree well.

In this section, we do not present our results on the comparison of SLBC_cci v0 GRACE ocean mass solutions with sum of SLBC_cci v0 mass components as Section 2.2 has already discussed this in detail using the updated (v0.3) GRACE solutions.

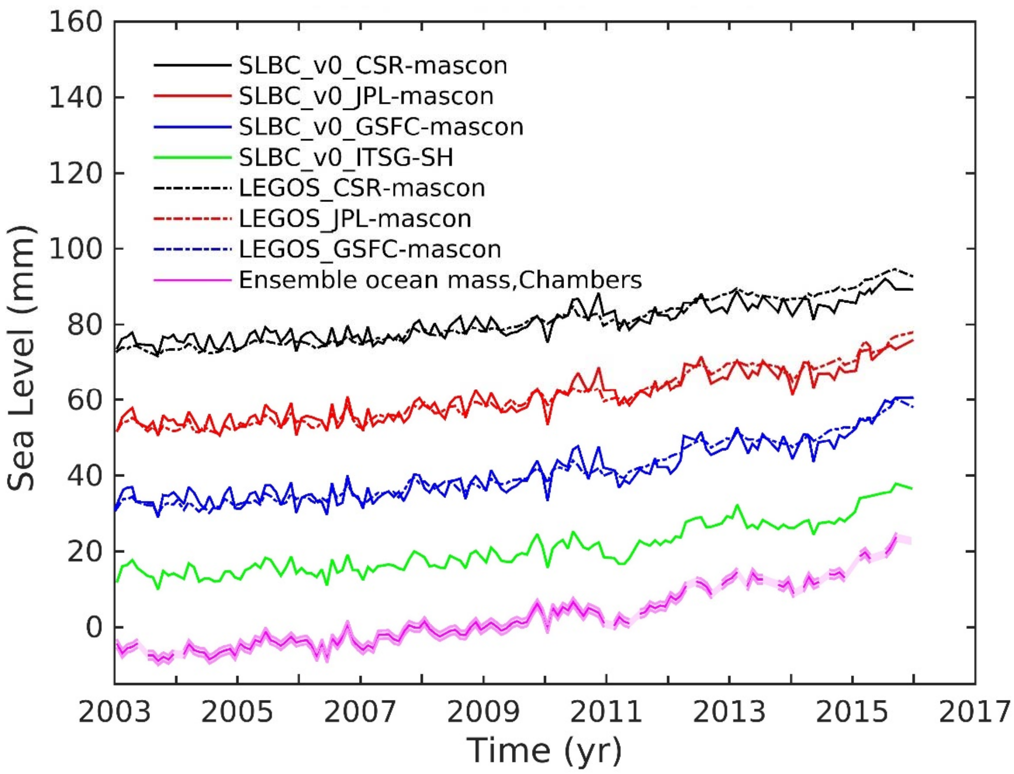

Figure 3.7: GRACE ocean mass variations over 2003-2015 from SLBC_cci_v0, LEGOS and Chambers solutions.

Table 3.2: Trend values of global mean ocean mass from GRACE (in mm/yr)

		2003-2015	2003-2011
SLBC_cci_v0	CSR Mascon	TBE	TBE
	JPL Mascon	1.51	1.18
	GSFC Mascon	1.73	1.18
	ITSG Spherical Harmonics	1.53	1.03
LEGOS	CSR Mascon	1.56	1.26
	JPL Mascon	1.78	1.30
	GSFC Mascon	1.93	1.33
Chambers	CSR Spherical Harmonics	2.05	1.56
	JPL Spherical Harmonics	1.95	1.4
	GFZ Spherical Harmonics	2.1	1.57
	Ensemble Mean	2.03	1.51

3.4 Sea level budget closure analysis over 2003-2015; Synthesis

As mentioned in the introductory part, we performed the sea level budget closure analysis over 2003-2015 only using two approaches:

(1) by comparing observed GMSL first with the sum of individual sea level components and

(2) comparing observed GMSL with the sum of steric and GRACE based ocean mass.

3.4.1 Sea level budget based on sum of components for the mass contributions and steric effect

Figure 3.8a displays the global mean sea level budget estimated as the sum of individual SLBC_cci_v0 sea level components superimposed to the observed altimetry based global mean sea level time series over 2003-2015 and its corresponding residual in Figure 3.8b. The global mean sea level trend obtained as the sum of individual SLBC_cci_v0 components over 2003-2015 accounts to 2.92±0.14 mm/yr whereas the observed altimetry based global mean sea level trend value accounts to 3.36±0.15 mm/yr leaving a residual of 0.44 mm/yr. The uncertainty for the trend from sum of SLBC_cci_v0 is estimated as the quadratic sum of given uncertainty estimate for each component wherever available.

Over 2003-2015, the non-closure value of 0.44 mm/yr is already quite promising considering that the SLBC_cci data sets used here are only the version 0. Furthermore, uncertainty estimations have not yet been calculated for all the sea level components. This is a major task that will be dealt with as the SLBC_cci project progresses.

Table 3.3 summarizes trend values for the observed GMSL and sum of components over 2003-2015 with their corresponding residuals. Trend uncertainty for the sum of components is estimated as the quadratic sum of given uncertainty estimate for each component wherever available.

Table 3.3: Observed GMSL trend compared with sum of components trend over 2003-2015. Residual trends are also given.

	2003-2015 Trend (mm/yr)	
	Dieng et al., 2017	**SLBC_cci_v0**
Observed GMSL	3.36±0.15	
Sum of components	3.19±0.11	2.92±0.14

Residual	0.17	0.44

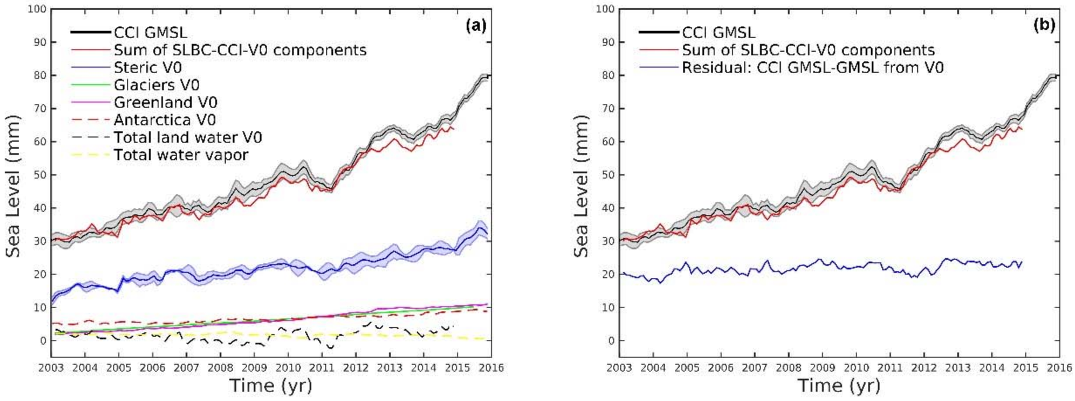

Figure 3.8: (a) Observed GMSL superimposed with the GMSL estimated from the sum of SLBC_cci_v0 sea level components over 2003-2015. The individual components are also plotted. (b) Observed GMSL superimposed with the GMSL estimated from the sum of SLBC_cci_v0 sea level components and the corresponding residual (observed GMSL minus sum of components) over 2003-2015.

3.4.2 Sea level budget using GRACE ocean mass and steric component

Over 2003-2015 time period corresponding to the Argo/GRACE era, the individual mass components can be replaced by ocean mass directly observed by GRACE as explained in the introduction. Therefore over this time period, we also perform the sea level budget using each of the three SLBC_cci_v0 GRACE ocean mass products with the aim of determining which of the SLBC_cci_v0 GRACE product produces best closure of the sea level budget.

Figure 3.9 displays the observed global mean sea level time series superimposed with the global mean sea level estimated as the sum of steric and GRACE ocean mass and corresponding residuals ($GMSL_{observed}$-$GMSL_{(steric+GRACE)}$).

From Figure 3.9 we observe that among the three SLBC_cci_v0 GRACE ocean mass products, in terms of linear trend, the global mean sea level estimated using the SLBC_cci_v0_GSFC_mascon time series agrees well with the observed GMSL (cf. Figure 3.9b).

The trend value corresponding to global mean sea level estimated using SLBC_cci_v0_GSFC_mascon accounts to 2.81 mm/yr (Table 3.4). Of the three SLBC_cci _v0 products, the trend estimated from this product is the closest to the observed GMSL. This is also evident from the residuals plotted (also see Figure 3.10 for comparison of residuals) that show that GSFC has least value among the three products (being 0.5 mm/yr) and the least RMS

(3.03 mm). More information on individual trend values, residuals is summarized in Table 3.4. It is however the Chambers GRACE ocean mass (trend = 3.13 mm/yr, residual = 0.15 mm/yr and RMS = 2.32) that provide best closure of the sea level budget. If we consider only the 2003-2011 time span, residual trends do not reduce significantly when compared to 2003-2015 except in the case of SLBC_cci_v0 JPL data (Table 3.4).

This preliminary analysis shows differences in the various GRACE ocean mass products used in the sea level budget. However, no specific problem has been identified that would explain these differences. While a possible suspect could be the data gaps since 2012, our results show only minor amelioration when data after 2011 is eliminated in the budget analysis. The future versions of GRACE ocean mass product should therefore work on identifying the causes of these differences (e.g. data processing and ocean mask application) and thereby solving such issues. One of these issues, signal leakage into the ocean due to land-ocean masks in SLBC_cci v0 GRACE products has already been addressed by WP221 and have henceforth used an updated version v0.3 with dedicated land-ocean masks for each GRACE ocean mass product in their mass budget analysis (Section 2). This has shown an improvement in their mass budget analysis and has reduced the differences (though not entirely) that we have shown between SLBC_cci v0 GRACE products and GRACE products from external sources. These improvements show the importance of using external data sources (and not only limiting to SLBC_cci products) as means of cross verification that helps in understanding issues that exist not only on SLBC_cci products but also on the external sources. Though the updated SLBC_cci v0.3 GRACE products could not be used (as explained in Section 3.1) in this present sea level budget closure analysis, these will be considered in future analysis.

Table 3.4: Trend and residual values of observed GMSL and sum of steric sea level plus GRACE ocean mass over 2003-2015.

		2003-2015		**2003-2011**	
		Trend (mm/yr) $GMSL_{(steric+GRACE)}$	**Residual (mm/yr)** $GMSL_{observed}$- $GMSL_{(steric+GRACE)}$	**Trend (mm/yr)**	**Residual (mm/yr)** $GMSL_{observed}$- $GMSL_{(steric+GRACE)}$
SLBC_cci_v0	CSR Mascon	N/A	N/A	N/A	N/A
	JPL Mascon	2.60	0.69	2.06	0.46
	GSFC Mascon	2.81	0.5	2.01	0.51
	ITSG Spherical Harmonics	2.61	0.67	1.88	0.65

Chambers	Ensemble Mean	3.13	0.15	2.36	0.16

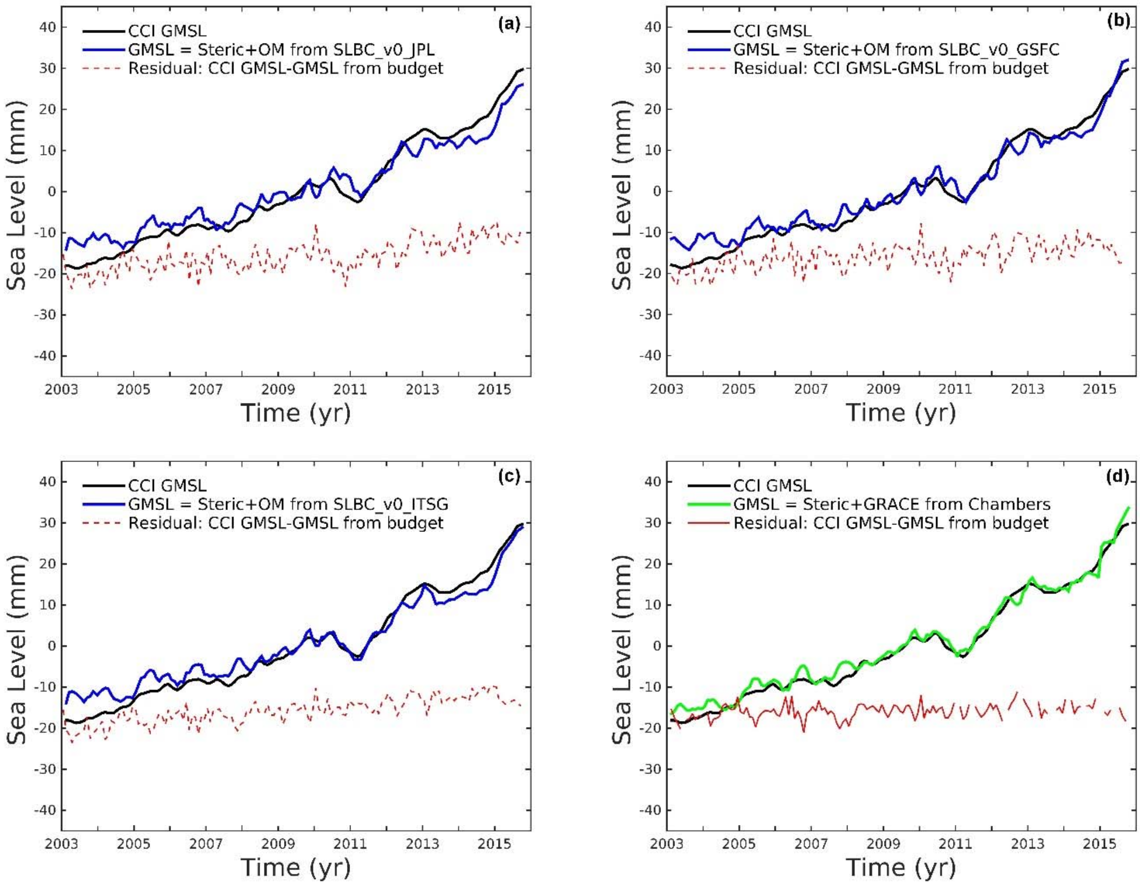

Figure 3.9: Comparison of global mean sea level time series estimated from SLBC_cci_v0 GRACE products (a) SLBC_cci_v0_JPL, (b) SLBC_cci_v0_GSFC, (c) SLBC_cci_v0_ITSG and from (d) Chambers ensemble mean with observed GMSL. Their corresponding residuals ($GMSL_{observed}$-$GMSL_{(steric+GRACE)}$) are also plotted with an arbitrary offset for clarity.

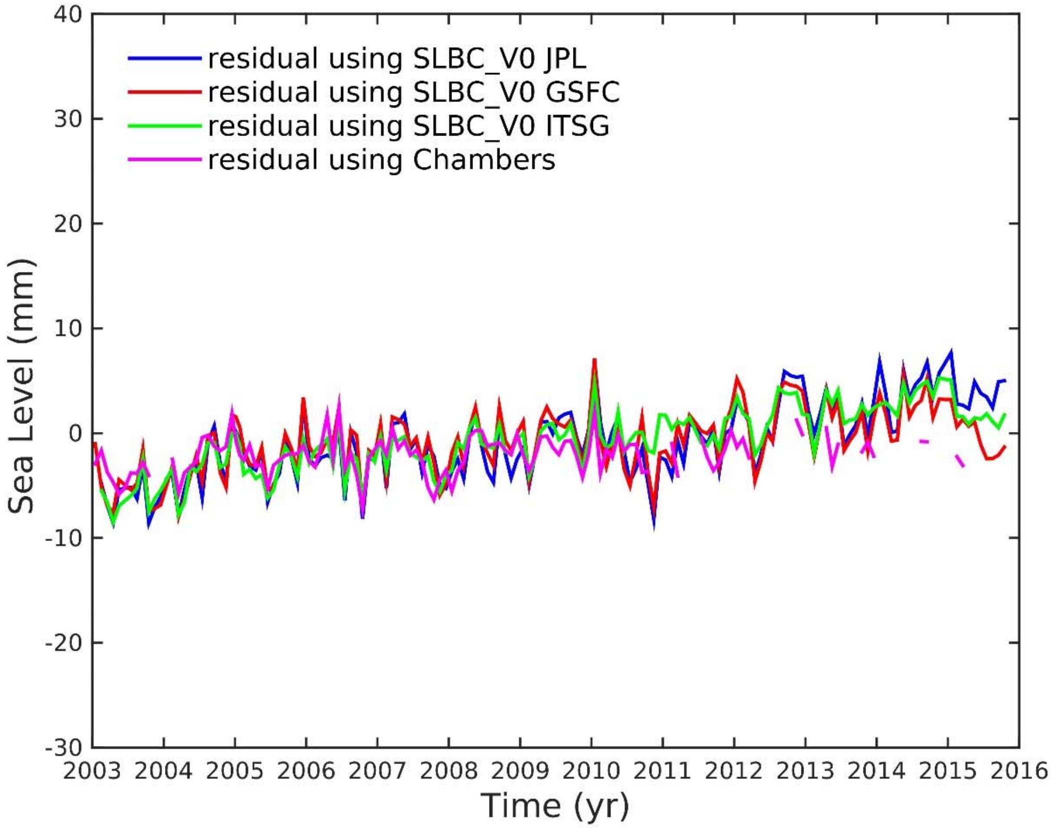

Figure 3.10: Residual time series obtained as the difference between observed GMSL and sum of steric sea level + GRACE ocean mass. Each curve is estimated from one of the 4 GRACE datasets considered.

4 Arctic Ocean Sea Level Budget

4.1 Data update

Data are described in data documentation document D2.1.2, however some synthesis of data coverage, gridding, masks, etc. is given here as part of this assessment.

Datasets used for this preliminary budget assessment are grid_sla_aviso (1993–2015), grid_sla_CCI_V2_0 (1993–2015, Figure 4.1c), and DTU_Arc_SLA (1992/9–2014/8, Figure 4.1b) for sea level, and data_grid_steric_EN4 (1990–2013, Figure 4.2b) for observed steric sea level change, and the four files EWH_OcMassChangeGrid_*_SLBC_1x1 (CSR 2002/4–2016/6; GSFC 2003/1–2016/3; ITSG 2002/8–2016/12; JPL 2002/4–2016/6, Figure 4.3a) for ocean mass. The model system TOPAZ provides both sea level and steric change in topazssh20032015 and topazstht20032015 (Figure 4.1a, Figure 4.2a), respectively (2003–2015). Other data sets were not applicable to Arctic sea level budget assessment.

For version 0, 66°N is chosen as border of the Arctic budgets, and all sets were cropped at this latitude. Regridding or subsampling was necessary for some sets in order to arrive at the recently agreed grid with cell-center points at *lon=[0.5:1:359.5]* and *lat=[66.5:1:89.5]*. DTU_Arc_SLA was simply subsampled from *lon=[0:0.5:360]* and *lat=[66:0.5:88]* to this grid and empty cells were added for the two northernmost latitudes, while data_grid_steric_EN4 was linearly interpolated from its *lon=[1:1:360]* and *lat=[66:1:89]* grid (hence leaving the northernmost line of cells empty). The TOPAZ data were subsampled from *lon=[-180:0.125:180]* and *lat=[66:0.125:90]*; i.e., at every eighth point delivered, and shifted in longitude to the desired 0.5–359.5 range.

A common land mask was made from the LAND_MASK.CRIv01 and adapted to the standard grid by marking grid cells with any land cells inside as land (taking into account the different spatial resolution of the grids, exactly 4 cells of LAND_MASK.CRIv01 were combined to 1 cell of our grid). All datasets were subjected to this mask, regardless of any pre-existing masking done.

Trends were found at each grid point by fitting a 1st degree polynomial to the series. In this assessment only the period 2003–2015 is considered. The fitting is done on full number of years only, to avoid seasonal effects. In order to limit the amount of spurious trends due to lack of data, criteria are applied for total amount of time points with data, as well as for amount of data in each quarter of the total time period. The criterion used in the result presented here is at least 80% months with data in total and at least 10% in each quarter. The sensitivity to this will be discussed below. (Note that this does not take care of any seasonal biases from missing data, an assessment of which will be done in later versions.)

The area of each grid cell of the standard grid was calculated as the surface area of the latitude-longitude quadrangle of the cell edges on a GRS-80 reference ellipsoid. This area matrix is used for all area weighting.

The total integrated trends were calculated as area weighted integrals of each cell's trend, over the ocean region north of 66°N. Cells with no trend are not part of the integral, which causes the overall trends to be biased towards the regions covered.

4.2 Budget assessment

For version 0 the assessment covers the region north of 66°N and trends were calculated for the time period 2003–2015, due to the various space and time coverage in v0 data.

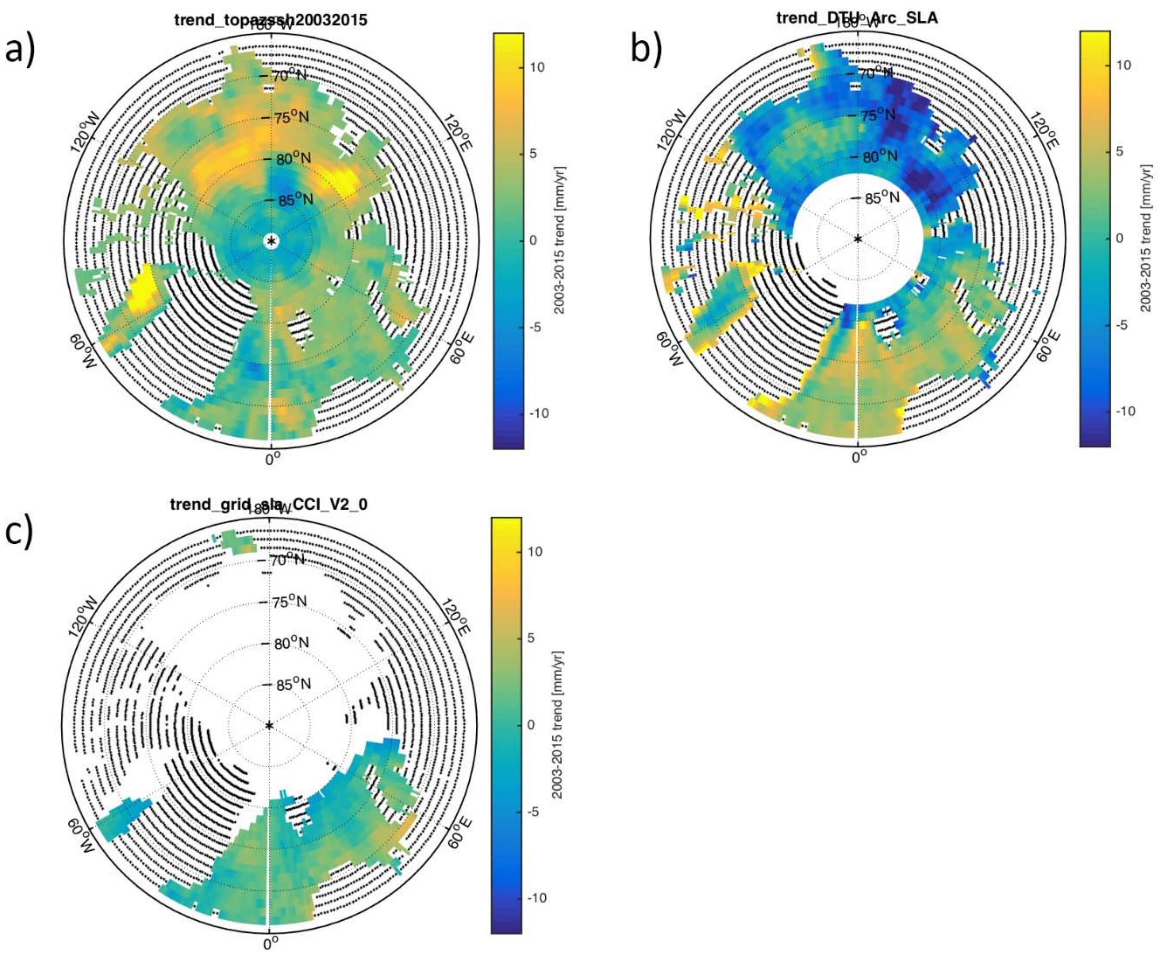

Figure 4.1: Trend patterns for sea level height change, 2003–2015, for (a) TOPAZ SSH, (b) DTU Arctic SLA, (c) CCI sea level. Black dots/circles mark the cells masked with the common land mask. Blank cells are cells with missing data (by the data coverage criterion or masked in data source).

For the TOPAZ runs, trends are 3.0 mm/yr for SSH and 1.2 mm/yr for the steric contribution. The sea level trends in CCI v2 is 0.8 mm/yr, in AVISO 1.9 mm/yr, and in DTU Arctic SLA -0.7 mm/yr. For EN4 the steric trend is 1.6 mm/yr. The sets CCI v2 and AVISO only have sufficient data to compute trends in the Nordic Seas and Barents Sea (not shown), hence the further discussion will be based on DTU Arctic SLA.

The ocean-mass trends diverge severely, as noted in the data documentation document D2.1.2. For the Arctic, CSR shows 1.5 mm/yr, ITSG -4.5 mm/yr, JPL 4.5 mm/yr, and GSFC 5.4 mm/yr. From the trend maps (not shown) it is clear that CSR and ITSG are influenced by mass loss on land (GrIS and Canadian Archipelago), while JPL and GSFC do not show fingerprints from those land based changes. The two latter are also the most consistent, although somewhat high compared to the sea level trends.

The TOPAZ trends of sea level and steric height leave 1.8 mm/yr to mass changes. The observed changes of sea level and steric change, DTU and EN4, on the other hand, imply a negative mass change of -0.8 mm/yr, since the steric estimate is higher than the sea level change. However, as mentioned, the two ocean mass products with the least land contamination are strongly positive.

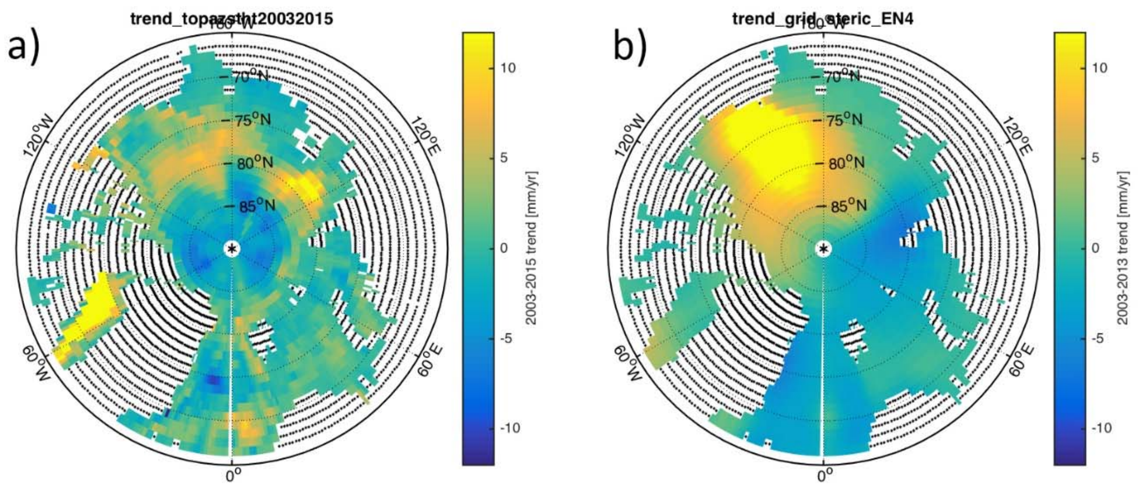

Figure 4.2: Trend patterns for steric height changes, 2003–2015, for (a) TOPAZ steric height, (b) EN4 steric height. Black dots/circles mark the cells masked with the common land mask. Blank cells are cells with missing data (by the data coverage criterion or masked in data source).

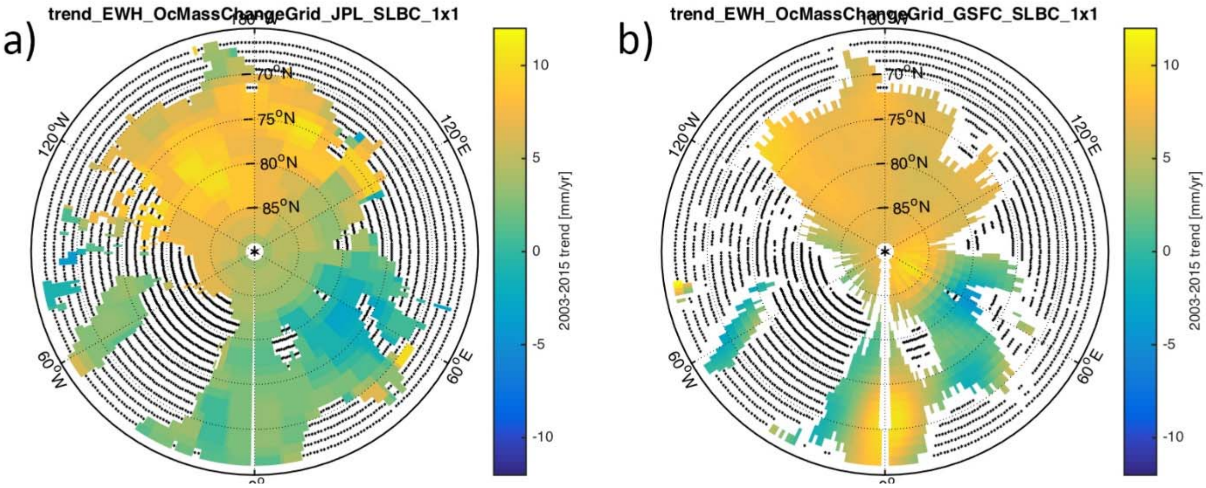

Figure 4.3: Trend patterns for ocean mass changes, 2003–2015, from (a) JPL, (b) GSFC. Black dots/circles mark the cells masked with the common land mask. Blank cells are cells with missing data (by the data coverage criterion or masked in data source).

4.3 Discussion

The v0 data has very different coverage. This leaves a full and consistent budget assessment to the next version. Also, with the existing methodological limitations, it makes no sense to assess uncertainties in this version of the datasets.

The criterion for time series coverage before making trends reduces the number of grid cells with trends. In DTU Arctic SLA there is little sensitivity to lowering the criteria below 80%/10% (total coverage/coverage in each grid), the overall Arctic sea level trend rounds off to -0.7 mm/yr in all cases. The sets CCI v2 and AVISO are sensitive to lowering the criteria and trends are lowered as more of the negative trending Arctic Ocean and Siberian shelves become included in the integral (e.g., sinks to -0.2 and 1.1 mm/yr, respectively, as the criteria are lowered to 50%/10%). The TOPAZ, EN4 steric height, and the ocean mass sets have no missing data, so their trends are robust w.r.t. data coverage.

The total budgets are of a very preliminary character. The apparent discrepancies can be due to several methodological issues, such as lacking inclusion for the areas without data coverage, to issues related to generation of the data sets involved. See for instance the uncovered polar region or the large spread in the ocean mass trends.

The CCI V2 and AVISO datasets both contain the IB correction for atmospheric pressure whereas this is not the case for the DTU dataset due to uncertainties in the quality of the IB correction in the Arctic. More investigation into this correction will be performed for the next iteration.

5 References

A, G., Wahr, J., and Zhong, S. (2013): Computations of the viscoelastic response of a 3-D compressible Earth to surface loading: an application to Glacial Isostatic Adjustment in Antarctica and Canada, *Geophys. J. Int.*, 192, 557–572, doi: 10.1093/gji/ggs030.

Ablain, M., J. F. Legeais, P. Prandi, M. Marcos, L. Fenoglio-Marc, H. B. Dieng, J. Benveniste, and A. Cazenave (2017): Altimetry-based sea level at global and regional scales, *Surv. Geophys.*, 38, 7–31, doi: 10.1007/s10712-016-9389-8.

Bergmann-Wolf, I., Zhang, L., and Dobslaw, H. (2014): Global Eustatic Sea-Level Variations for the Approximation of Geocenter Motion from Grace. *Journal of Geodetic Science*, 4(1). doi:10.2478/jogs-2014-0006.

Bloßfeld, M., Müller, H., Gerstl, M., Štefka, V., Bouman, J., Göttl, F., and Horwath, M. (2015): Second-degree Stokes coefficients from multi-satellite SLR. *J. Geod.*, 89(9), 857–871. doi: 10.1007/s00190-015-0819-z.

Bruinsma, S.; Lemoine, J. M.; Gegout, P.; Biancale, R.; Bourgogne, S. (2014): *Updated Release 3 of the GRACE Gravity Solutions from CNES/GRGS*. AGU Fall Meeting, San Francisco.

Chambers, D. P. and Bonin, J. A. (2012): Evaluation of Release-05 GRACE time-variable gravity coefficients over the ocean, *Ocean Sci.*, 8, 859–868, doi: 10.5194/os-8-859-2012.

Chambers, D.P., Cazenave, A., Champollion D., Dieng, H., Llovel, W., Forsberg, R. von Schuckmann, K., Wada, Y. (2017): Evaluation of the Global Mean Sea Level Budget between 1993 and 2014. Surv Geophys (2017) 38:309–327 DOI 10.1007/s10712-016-9381-3

Cheng, M. K., Ries, J. C., and Tapley, B. D. (2013a): Geocenter Variations from Analysis of SLR Data. In Z. Altamimi, and X. Collilieux (Eds.): *Reference Frames for Applications in Geosciences* (pp. 19–25). International Association of Geodesy Symposia, 138. Springer Berlin Heidelberg.

Cheng, M., Tapley, B. D., and Ries, J. C. (2013b): Deceleration in the Earth's oblateness. *J. Geophys. Res. Solid Earth*, 118(2), 740–747. doi:10.1002/jgrb.50058.Cogley, J. G. (2009): Geodetic and direct mass-balance measurements: Comparison and joint analysis, *Ann. Glaciol.*, 50(50), 96–100.

Cogley, J. G. (2009). Geodetic and direct mass-balance measurements: comparison and joint analysis. Annals of Glaciology, 50(50), 96-100.

Decharme, B., Brun, E., Boone, A., Delire, C., Le Moigne, P., and Morin, S. (2016): Impacts of snow and organic soils parameterization on northern Eurasian soil temperature profiles simulated by the ISBA land surface model, *The Cryosphere*, 10, 853-877, doi: 10.5194/tc-10-853-2016.

Dee, D. P., et al. (2011): The ERA-Interim reanalysis: Configuration and performance of the data assimilation system, *Q. J. R. Meteorol. Soc.*, 137, 553–597, doi: 10.1002/qj.828.

Dieng, H. B., A. Cazenave, K. von Shuckmann, M. Ablain, and B. Meyssignac (2015): Sea level budget over 2005–2013: Missing contributions and data errors, *Ocean Sci.*, 11, 789–802, doi: 10.5194/os-11-789-2015.

Dieng H., Cazenave A., Meyssignac B. and Ablain M. (2017): New estimate of the current rate of sea level rise from a sea level budget approach, *Geophys. Res. Lett.*, 44, doi: 10.1002/2017GL073308, 2017.

Döll, P., M. Fritsche, A. Eicker, and S. H. Mueller (2014a): Seasonal water storage variations as impacted by water abstractions: Comparing the output of a global hydrological model with GRACE and GPS observations, *Surv. Geophys.*, doi: 10.1093/gji/ggt485.

Döll, P., H. Mueller Schmied, C. Schuh, F. T. Portmann, and A. Eicker (2014b): Global-scale assessment of groundwater depletion and related groundwater abstractions: Combining hydrological modeling with information from well observations and GRACE satellites, *Water Resour. Res.*, 50, 5698–5720, doi: 10.1002/2014WR015595.

Forsberg R., Sørensen L., and Simonsen S. (2017): Greenland and Antarctica Ice Sheet Mass Changes and Effects on Global Sea Level, *Surv. Geophys.*, 38, 89-104, 7–31, doi:10.1007/s10712-016-9398-7.

Good, S. A., M. J. Martin, and N. A. Rayner (2013): EN4: Quality controlled ocean temperature and salinity profiles and monthly objective analyses with uncertainty estimates, *J. Geophys. Res. Oceans*, 118, 6704–6716, doi:10.1002/2013JC009067.

GUM (2008): Joint Committee for Guides in Metrology, 2008: Evaluation of measurement data - *Guide to the expressio3.1n of uncertainty in measurement*. Bureau International des Poids et Mesures, available from www.bipm.org/en/publications/guides/, pp. 130.

Ishii, M., M. Kimoto and M. Kachi (2003): Historical ocean subsurface temperature analysis with error estimates, *Mon. Weather Rev.*, 131, 51-73

Ishii, M., and M. Kimoto (2009): Reevaluation of historical ocean heat content variations with time-varying XBT and MBT depth bias corrections, *J. Oceanogr.*, *65*(3), 287–299, doi:10.1007/s10872-009-0027-7.

Johnson, G. C., and Chambers, D. P. (2013). Ocean bottom pressure seasonal cycles and decadal trends from GRACE Release-05: Ocean circulation implications. *J. Geophys. Res.* 118(9), 4228-4240.

Leclercq, P. W., J. Oerlemans, and J. G. Cogley (2011): Estimating the glacier contribution to sea-level rise for the period 1800–2005, *Surv. Geophys.*, 32, 519–535.

Legeais, J.-F., Ablain, M., Zawadzki, L., Zuo, H., Johannessen, J.A., Scharffenberg, M.G., Fenoglio-Marc, L., Fernandes, M.J., Andersen, O B., Rudenko, S., Cipollini, P., Quartly, G.D., Passaro, M., Cazenave, A., and Benveniste, J. (2018): An improved and homogeneous altimeter sea level record from the ESA Climate Change Initiative, Earth Syst. Sci. Data, 10, 281-301, https://doi.org/10.5194/essd-10-281-2018.

Levitus S., et al. (2012): World ocean heat content and thermosteric sea level change (0–2000 m), 1955–2010. *Geophys. Res. Lett.*, 39, L10603. doi: 10.1029/2012GL051106.

MacIntosh, C. R., Merchant, C. J., and von Schuckmann, K. (2017): Uncertainties in steric sea level change estimation during the satellite altimeter era: concepts and practices. *Surveys in Geophysics*, 38 (1). ISSN 0169-3298 doi: 10.1007/s10712-016-9387-x .

Marzeion, B., P. W. Leclercq, J. G. Cogley, and A. H. Jarosch (2015): Brief communication: Global reconstructions of glacier mass change during the 20th century are consistent, *Cryosphere*, 9, 2399–2404, doi:10.5194/tc-9-2399-2015.

Müller Schmied, H., Eisner, S., Franz, D., Wattenbach, M., Portmann, F. T., Flörke, M., & Döll, P. (2014). Sensitivity of simulated global-scale freshwater fluxes and storages to input data, hydrological model structure, human water use and calibration. Hydrology and Earth System Sciences, 18(9), 3511-3538.

Peltier, W. R. (1994): Ice Age Paleotopography. *Science*, 265(5169), 195–201. doi:10.1126/ science.265.5169.195.

Peltier, W. R., Argus, D. F., and Drummond, R. (2015): Space geodesy constrains ice age terminal deglaciation: The global ICE-6G_C (VM5a) model: Global Glacial Isostatic Adjustment. *J. Geophys. Res. Solid Earth*, 120(1), 450–487. doi:10.1002/2014JB011176.

Rietbroek, R., Brunnabend, S.-E., Kusche, J., Schröter, J., and Dahle, C. (2016): Revisiting the contemporary sea-level budget on global and regional scales. *Proc. Natl. Acad. Sci. USA*, 113(6), 1504–1509. doi:10.1073/pnas.1519132113.

Shepherd, A., et al. (2012): A reconciled estimate of ice-sheet mass balance, *Science*, 338, 1183–1189.

Sun, Y., Riva, R. E. M., and Ditmar, P. (2016): Optimizing estimates of annual variations and trends in geocenter motion and J2 from a combination of GRACE data and geophysical models. *J. Geophys. Res. Solid Earth*, 121(11), 8352–8370. doi:10.1002/2016JB013073.

Swenson, S., Chambers, D., and Wahr, J. (2008): Estimating geocenter variations from a combination of GRACE and ocean model output. *J. Geophys. Res.*, B113, B08410. doi:10.1029/2007JB005338.

von Schuckmann, K., and P.-Y. Le Traon (2011): How well can we derive Global Ocean Indicators from Argo data?, *Ocean Sci.*, 7, 783–791, doi: 10.5194/os-7-783-2011.

Wada, Y., M.-H. Lo, P. J. F. Yeh, J. T. Reager, J. S. Famiglietti, R.-J. Wu, and Y.-H. Tseng (2016): Fate of water pumped from underground and contributions to sea level rise, Nat. Clim. Change, doi: 10.1038/NCLIMATE3001.

Williams, S. D. P. (2003). The effect of coloured noise on the uncertainties of rates estimated from geodetic time series. Journal of Geodesy, 76(9-10), 483-494.

6 Annex

Data sets used in Dieng et al. (2017)

The data sets used in Dieng et al., 2017 for each of the sea level components are listed below:

- Observed GMSL: Ensemble mean of GMSL time series from 6 processing groups: AVISO (Validation and Interpretation of Satellite Oceanographic data), University of Colorado, NOAA (National Oceanographic and Atmospheric Administration), GSFC (Goddard Space and Flight Center) version 2, CSIRO (Commonwealth Scientific and Industrial Research Organization) and ESA-CCI (Climate Change Initiative).
- Steric sea level: For the period January 1993-December 2004, the following three data sets have been considered: the updated versions of Ishii and Kimoto (2009), NOAA data set (Levitus et al., 2012) and EN4 data set (Good et al., 2013). Over the recent years, these data sets integrate Argo data from IPRC (International Pacific Research center), JAMSTEC (Japan Agency for Marine-Earth Science and Technology) and SCRIPPS. Dieng et al., 2017 use an ensemble mean of all the above mentioned steric data.
- Glaciers: An ensemble mean of glacier contribution from Marzeion et al., 2015, Leclerq et al., 2011 and the updated R1501 version of Cogley et al., 2009.
- Greenland and Antarctica: Two ice sheet mass balance time series have been used: (1) the IMBIE (Ice sheet Mass Balance Intercomparison Exercise) time series (Shepherd et al., 2012) up to 2003 and the CCI products (Forsberg et al., 2017) beyond.
- Land waters: ISBA (Interaction Soil Biosphere Atmosphere)/TRIP (Total Runoff Integrating Pathways) hydrological model from MeteoFrance (Decharme et al., 2016) for the natural climate variability and Wada et al., 2016 for the anthropogenic component of land waters were considered.
- Atmospheric water vapor was accounted for using the ERA-Interim atmospheric reanalysis (Dee et al., 2011).

To estimate uncertainties, Dieng et al., 2017 performed a quadratic sum of errors associated with time series (if available in the data sets) and of the random dispersion of time series around the ensemble mean. If a dataset does not provide errors, only the random dispersion around the mean was considered.

The limitations of this approach need to be considered. In particular, the combination of uncertainties as the sum of squares is applicable only where the uncertainties are believed to be independent from each other. Therefore, while a sum of squares approach may be appropriate to produce a combined SSH uncertainty from e.g. GRACE mass and steric height, it is not expected to be appropriate when estimating total uncertainty from an ensemble of data products using common inputs, which might reasonably be considered to have correlated errors.

In the example case of multiple steric height datasets, the assumption that uncertainty estimates from different products are independent is problematic. For example, several steric data products (KVS, von Schuckmann and Le Traon, 2011; EN4, Good et al., 2013; IK, Ishii et al., 2003; see Figure 3.6), provide uncertainty estimates that include some measure of sampling uncertainty due to sparse coverage. One could reasonably expect that this component of the uncertainty would be correlated across datasets. If the total uncertainty only is reported, it is usually not possible a posteriori to separate this correlated components from other contributions to the total uncertainty.

Other sources of uncertainty may also be accounted for (e.g. von Schuckmann and Le Traon, 2011 also accounts for uncertainty associated with background climatology), therefore the assumption that uncertainty estimates for a particular product represents only the random data errors is incorrect.

Further, the assumption that the ensemble spread (systematic uncertainty?) is independent from the individual product uncertainties is also problematic – for example, one might expect a larger ensemble spread for sparser data coverage, but this would also become apparent in those datasets which account or sampling uncertainty in their own estimates. MacIntosh et al., 2017 provide a review of uncertainty sources accounted for in steric height data products.

The Guide to Uncertainty in Measurement (GUM, 2008) provides a framework for the propagation of uncertainty when there are correlated terms to consider (their Equation 16):

$$u_c^2(y) = \sum_{i=1}^{N} c_i^2 u^2(x_i) + \sum_{i=1}^{N-1} \sum_{j=i+1}^{N} c_i c_j u(x_i) u(x_j) r(x_i, x_j)$$

where c_i is the sensitivity coefficient of the i th term, $u(x_i)$ is the uncertainty associated with x_i and $r(x_i, x_j)$ is the correlation between x_i and x_j.

Thus, the sum of squares is a special case when all sensitivity coefficients (weights) are 1, and all off-diagonal correlation terms are zero i.e. the uncertainty estimates are independent. In all other cases, the relationship between uncertainty estimates must be known. While the principles are very simple, the execution is in practice complex.

In the absence of explicit knowledge of correlation terms, but where uncertainties might reasonably be expected to have some relationship, the quadratic sum provides a lower bound on the true uncertainty estimate (even without considering that many uncertainty terms are not accounted for at all). Where this is the case in this report, we have explicitly acknowledged the limitation.

A focus of the steric part of this project is to construct a component-wise uncertainty budget that explicitly accounts for terms in a single product that are correlated, and separates uncertainty in the final product into independent types. In principle, this provides not only a deepened understanding of uncertainty sources from in situ data, but has the potential to allow for combination with additional data – such as SST estimates, which may have partly correlated uncertainty structures.

If a dataset does not provide errors, only the random dispersion around the mean was considered.

End of document